Testing the cold dark matter model with gravitational lensing

Priyamvada Natarajan
Departments of Astronomy & Physics
Yale University

In Memoriam: Vera Rubin

New Directions in Theoretical Physics , January 11, 2017

Higgs Center Workshop, Edinburgh

Collaborators

- **CATS** Jean-Paul Kneib, Johan Richard, Mathilde Jauzac, Hakim Atek, Eric Jullo, Marceau Limousin, Harald Ebeling, Benjamin Clement, Eiichi Egami
- **ILLUSTRIS** Lars Hernquist, Mark Vogelsberger, Volker Springel and the Illustris collaboration
- Urmila Chadayammuri
- Anson D'Aloisio
- Massimo Meneghetti

Why clusters of galaxies?

- Uniquely offer constraints on dark matter and dark energy simultaneously
- Originally the objects that provided evidence for the existence of dark matter
- Two independent and compelling lines of evidence – dynamically (classical Newtonian view) and gravitational lensing (GR)

Understanding cluster-lenses

Lensing tests of dark matter

Mass profiles of clusters: concentration
Substructure: abundance, profiles, spatial distribution
Density profiles - inner and outer slopes
Shapes of dark matter halos
Higher order statistics: flexion, correlation function of substructure – pencil beam surveys, P(k)
Science by stacking

Lensing constraints on dark energy

Cosmography with strong lensing (CSL)
Triplet statistics

Lensing tests of the standard world model
Primordial Non-Gaussianity (Arc-statistics)
Growth of Structure and Structure Formation

Composition of the Cosmos

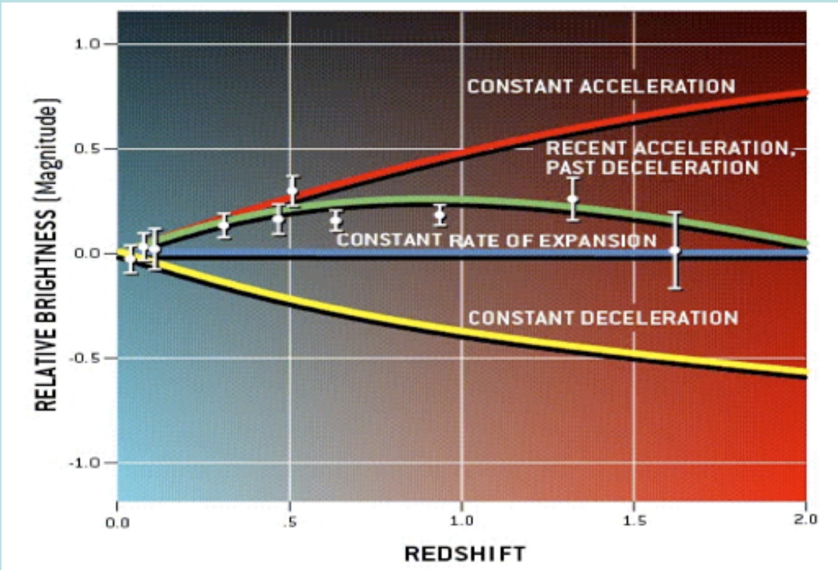

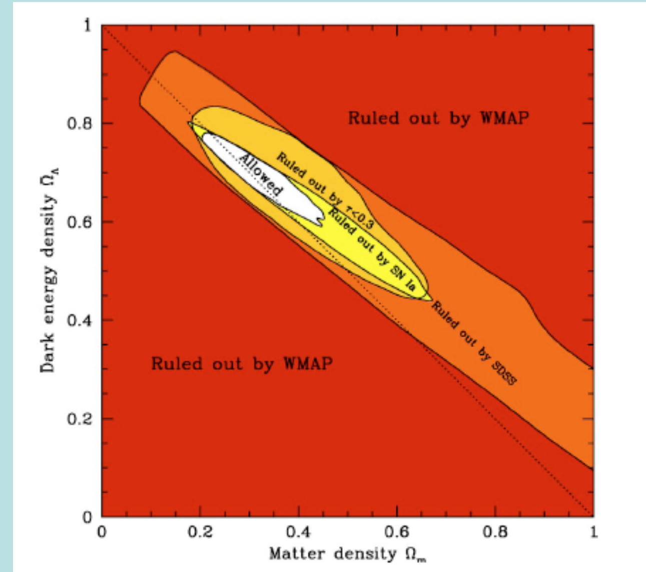

Compelling cosmological evidence for non-baryonic DM

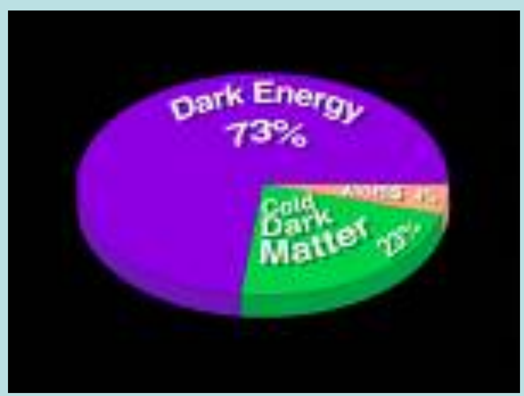

$\Omega_d h^2$ (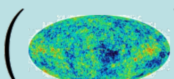) $= 0.113$

WIMPS: Weakly Interacting Massive Particles - the lightest neutralino, motivated by SUSY, mean scattering time-scale longer than Hubble time

AXIONS & WISPS: new mass windows being explored for axions and axion-like particles

Riess+ 98 Perlmutter +99;
Tegmark+ 03; Spergel+ 03; 06;
WMAP, SDSS, 2dF

Clusters: summary

Composition

~1 % of mass is in galaxies

~10 % of mass is hot gas

the rest is dark matter

- Understanding clusters

how much mass?

does light trace mass?

how is the dark matter distributed?

how granular is the dark matter?

Geller+; Rines+; Postman+ CLASH; Treu+; Starikova+; Newman+; Sand+; Bradac+; Williams+; de Lucia+; Hennawi+; Gladders+; Oguri+; Broadhurst+; for details see review Kneib & PN 11

Measuring lensing signals

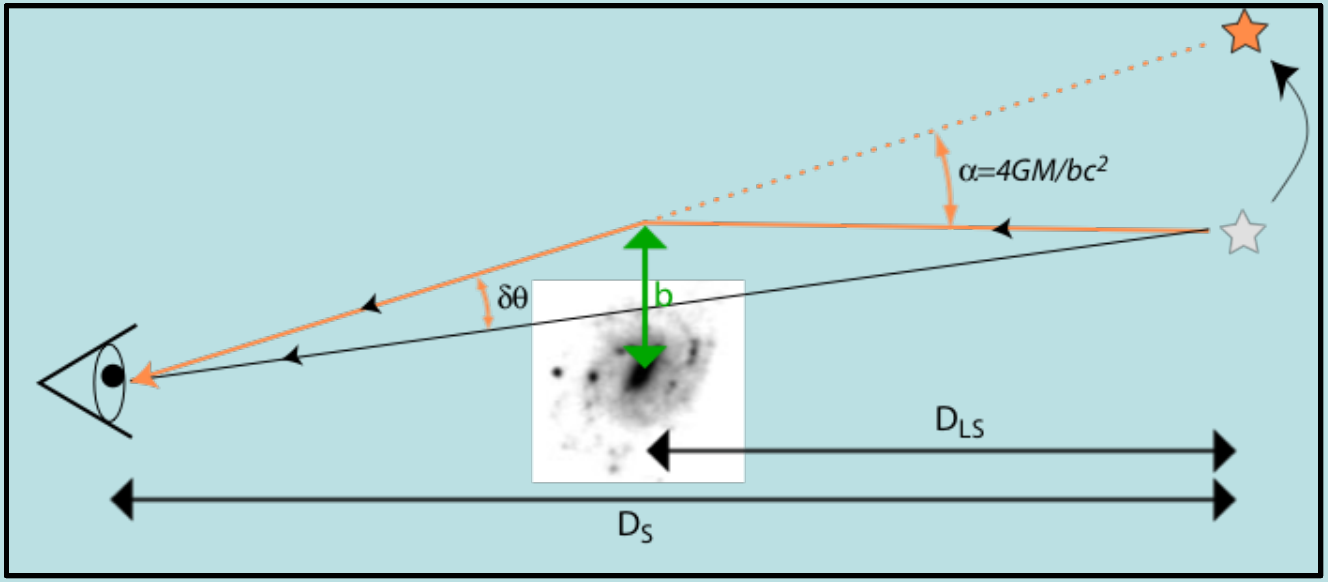

$$\delta\theta = \frac{4GM}{bc^2}\,\frac{D_{LS}}{D_S}$$

We observe this deflection angle (more precisely, gradients of the deflection angle).

Cosmology changes growth rate of mass structures in the Universe.

Cosmology changes the geometric distance factors.

The deflection is proportional to the mass

Blandford & Narayan 92; Schneider Ehlers & Falco 92; Bartelmann & Narayan 97; Kneib & PN 10

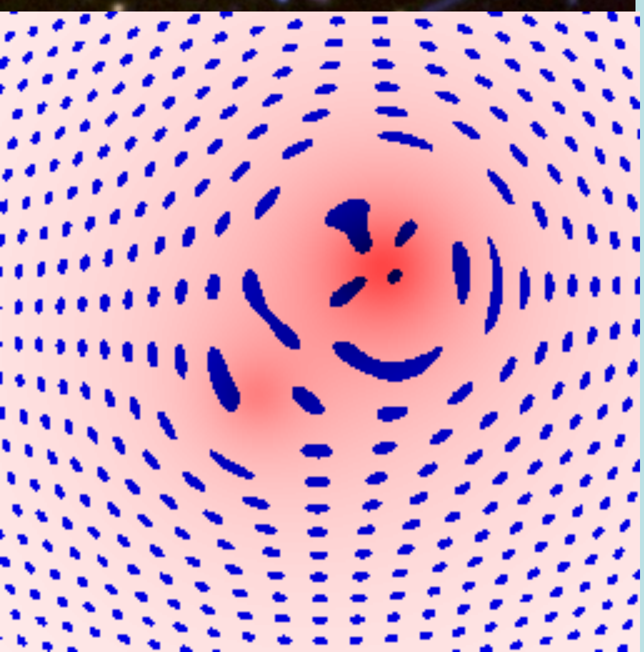

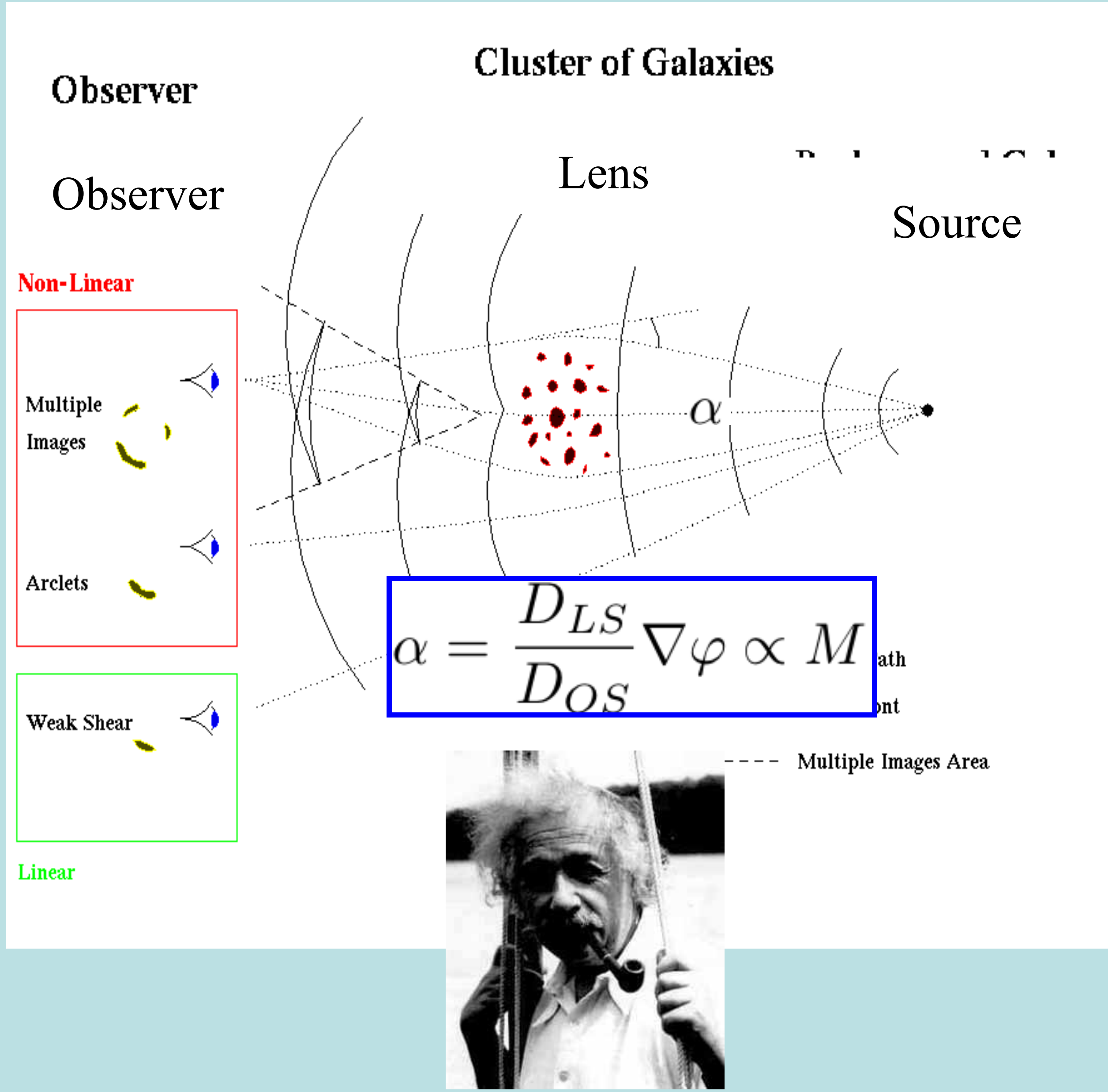

$$\alpha = \frac{D_{LS}}{D_{OS}} \nabla \varphi \propto M$$

Einstein radii at multiple source redshifts

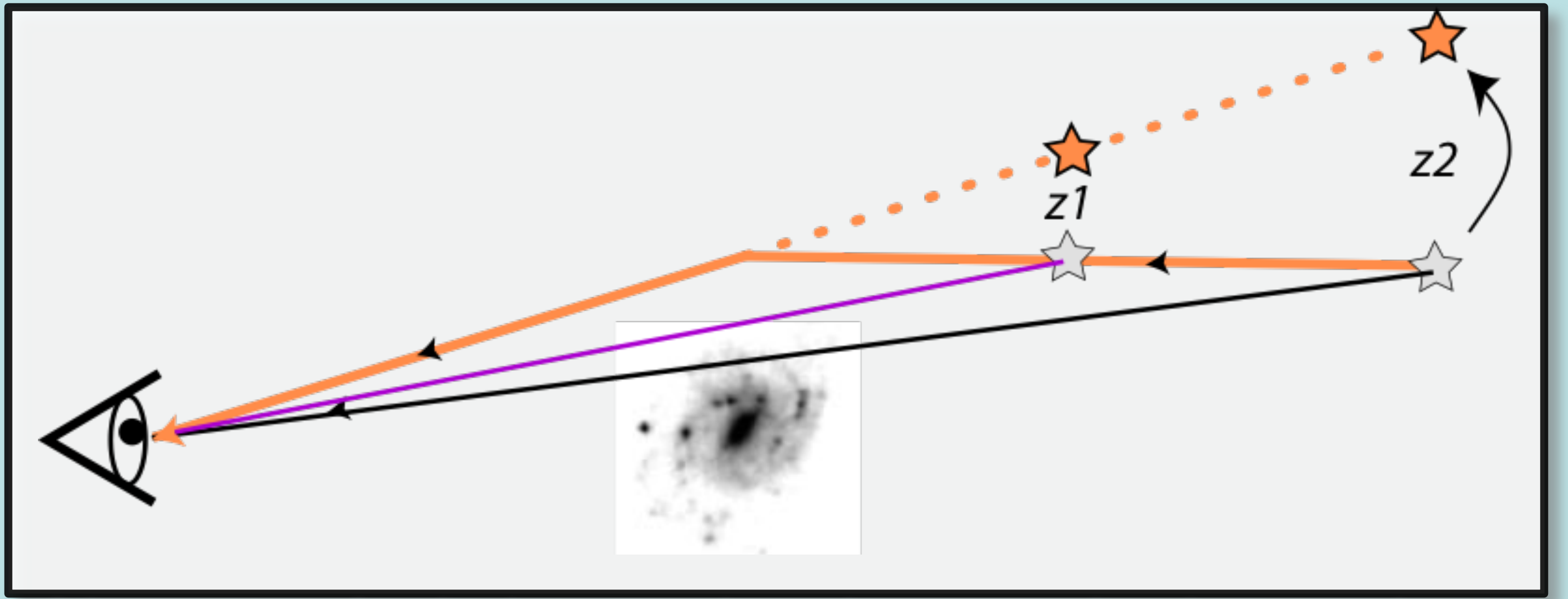

Ratio of the position of multiple images,depends on mass distribution and cosmological parameters

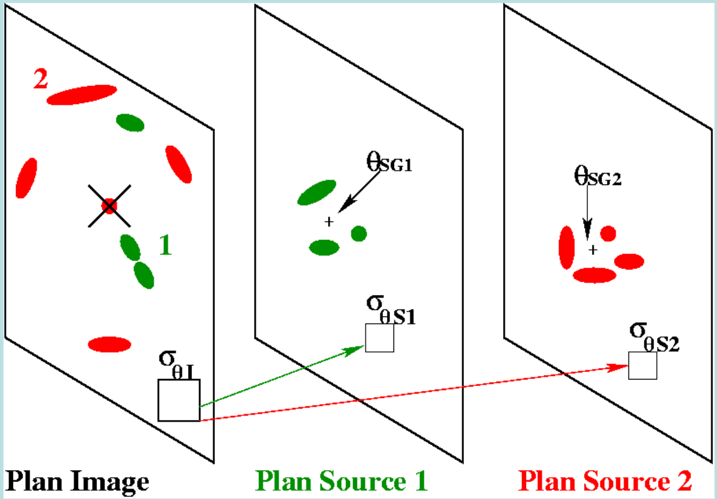

Cluster arcs and dark energy: Abell 1689

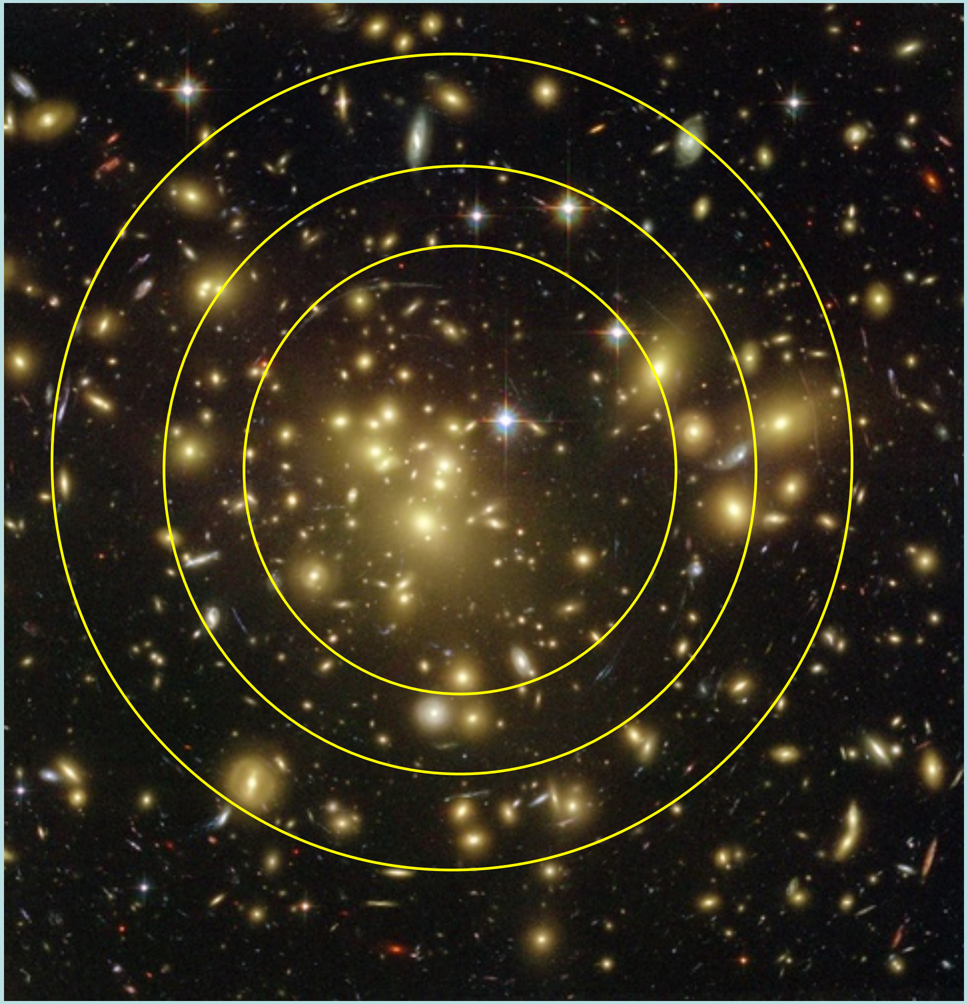

34 multiply imaged systems, 24 with measured redshifts

Broadhurst+ 05, Benitez+ 06; Halkola+ 06; Limousin, PN+ 07; Jullo+ 2010

How does this work?

ISOTHERMAL SPHERE LENS lens at $z = z_L$; sources at z_{S1} & z_{S2}

$$R_{E_1} = \frac{4ps^2}{c^2}\frac{D_{LS_1}}{D_{OS_1}} \qquad R_{E_2} = \frac{4ps^2}{c^2}\frac{D_{LS_2}}{D_{OS_2}}$$

$$D_{ij} \equiv f(z_i, z_j, \Omega_M, \Omega_x, w_x)$$

$$\frac{R_{E_1}}{R_{E_2}} = [\frac{D_{LS_1}}{D_{OS_1}}][\frac{D_{OS_2}}{D_{LS_2}}]$$

Obtained from data

Solve for cosmological parameters

- EXTENDING TO MORE COMPLICATED MASS PROFILES AND MORE MULTIPLY IMAGED SOURCES

Measuring lensing signals

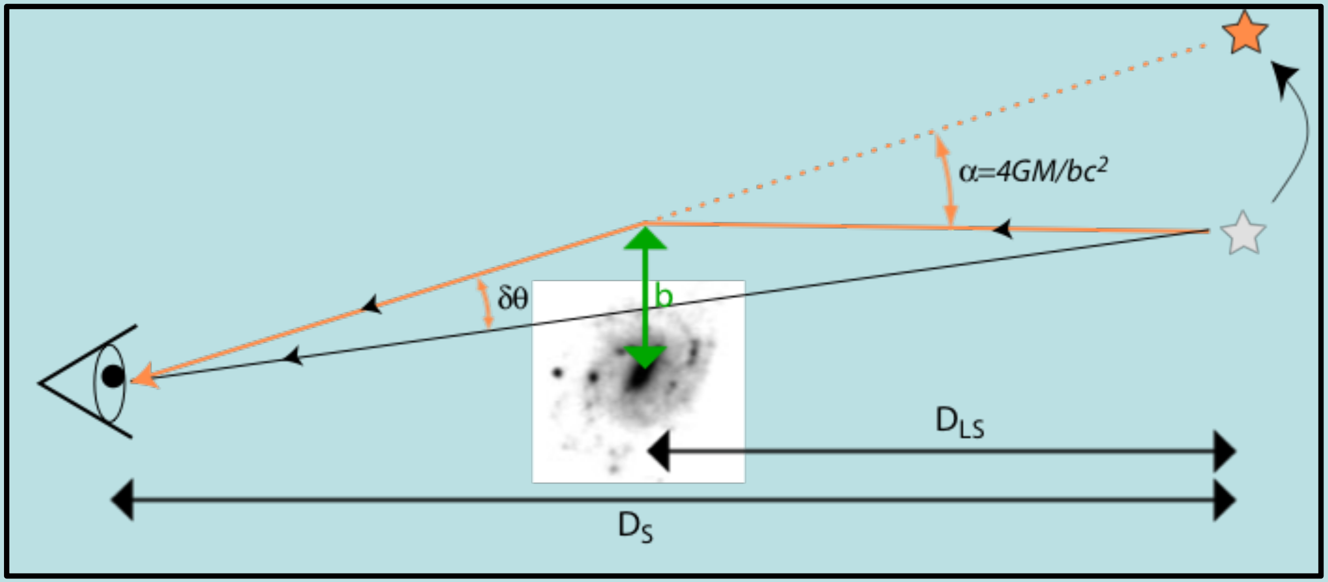

$$\delta\theta = \frac{4GM}{bc^2} \frac{D_{LS}}{D_S}$$

We observe this deflection angle (more precisely, gradients of the deflection angle).

Cosmology changes growth rate of mass structures in the Universe.

Cosmology changes the geometric distance factors.

The deflection is proportional to the mass

Blandford & Narayan 92; Schneider Ehlers & Falco 92; Bartelmann & Narayan 97; Kneib & PN 10

Strong lensing
multiple image geometries for an elliptical lens

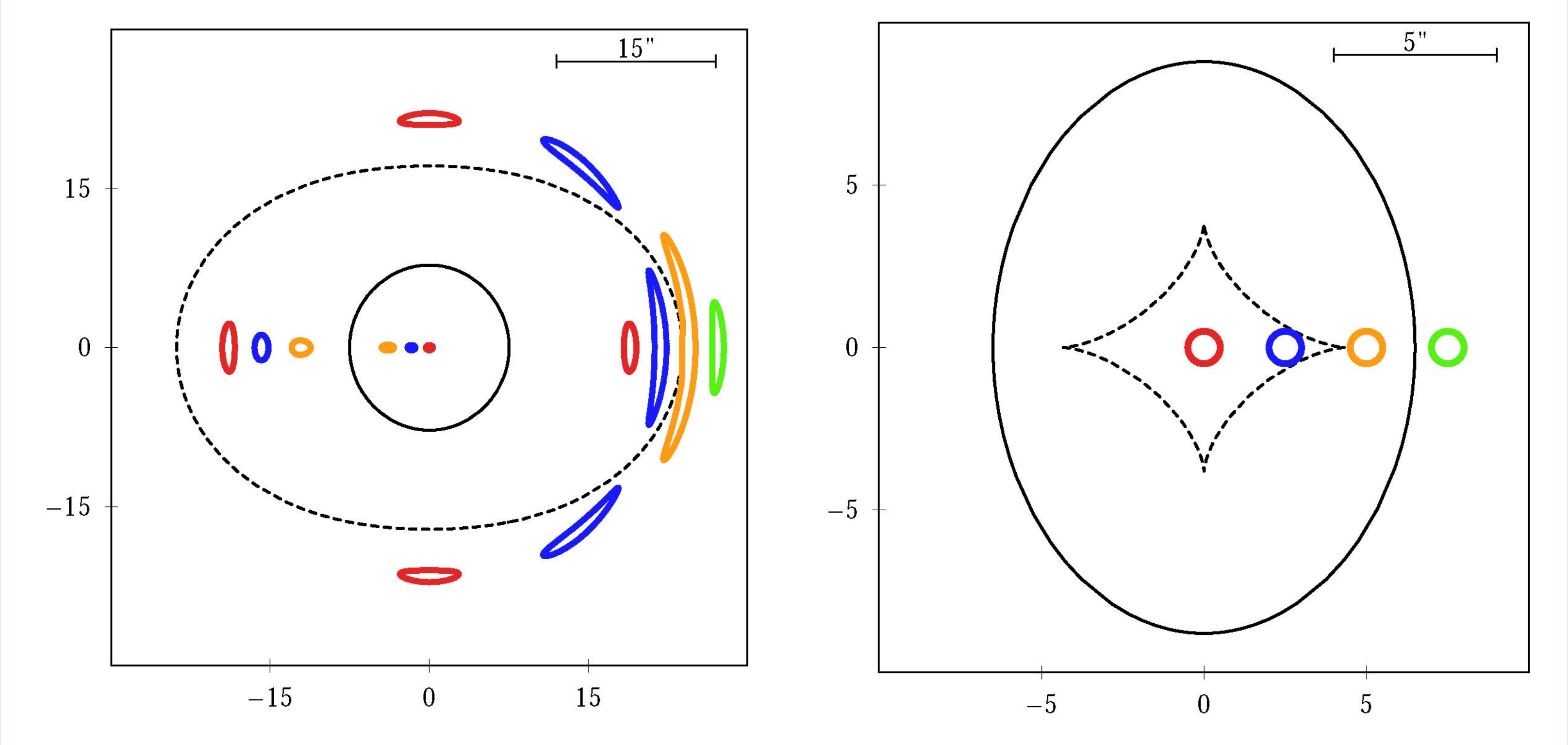

Image plane
critical curves

Source plane
caustics

Observing shapes of galaxies

$$e = \left[\frac{a^2 - b^2}{a^2 + b^2}\right] \cdot e^{2if}$$

in the weak lensing regime

$$e^{obs} = e^{\mathrm{int}} + g$$

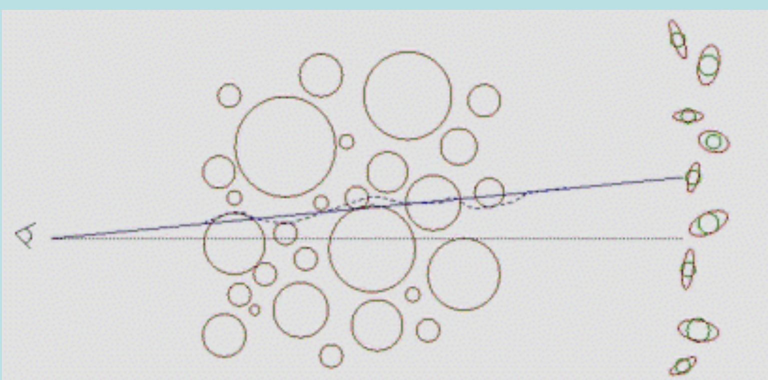

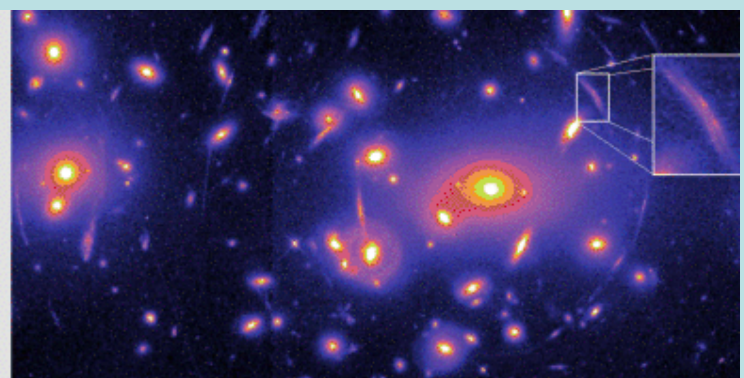

Lens Mapping

$$\mathcal{A}^{-1} = \begin{pmatrix} 1-\kappa-\gamma_1 & -\gamma_2 \\ -\gamma_2 & 1-\kappa+\gamma_1 \end{pmatrix}$$

Amplification matrix

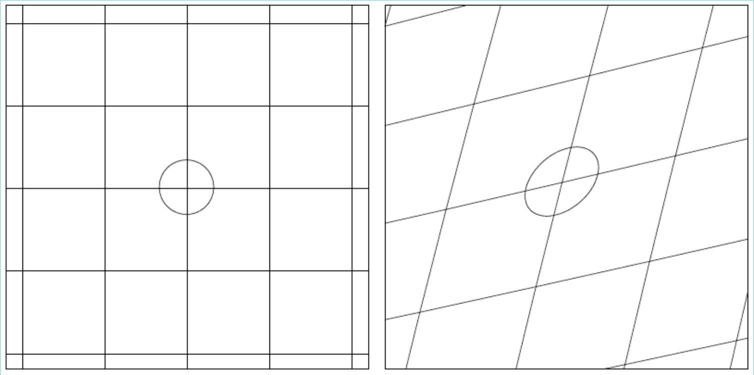

source image

convergence $\kappa = \Delta\varphi/2 = \Sigma/2\Sigma_{crit}$

shear $\gamma_1 = (\partial_{yy}\varphi - \partial_{xx}\varphi)/2 \qquad \gamma_2 = \partial_{xy}\varphi$

$$\Sigma_{\rm cr} = \frac{c^2}{4\pi G}\frac{D_{\rm s}}{D_{\rm d}D_{\rm ds}}$$
$$= 0.35\,{\rm g\,cm^{-2}}\left(\frac{D}{1\,{\rm Gpc}}\right)^{-1}$$

Reduced shear: measured quantity

$$g = \frac{\gamma}{1-\kappa}$$

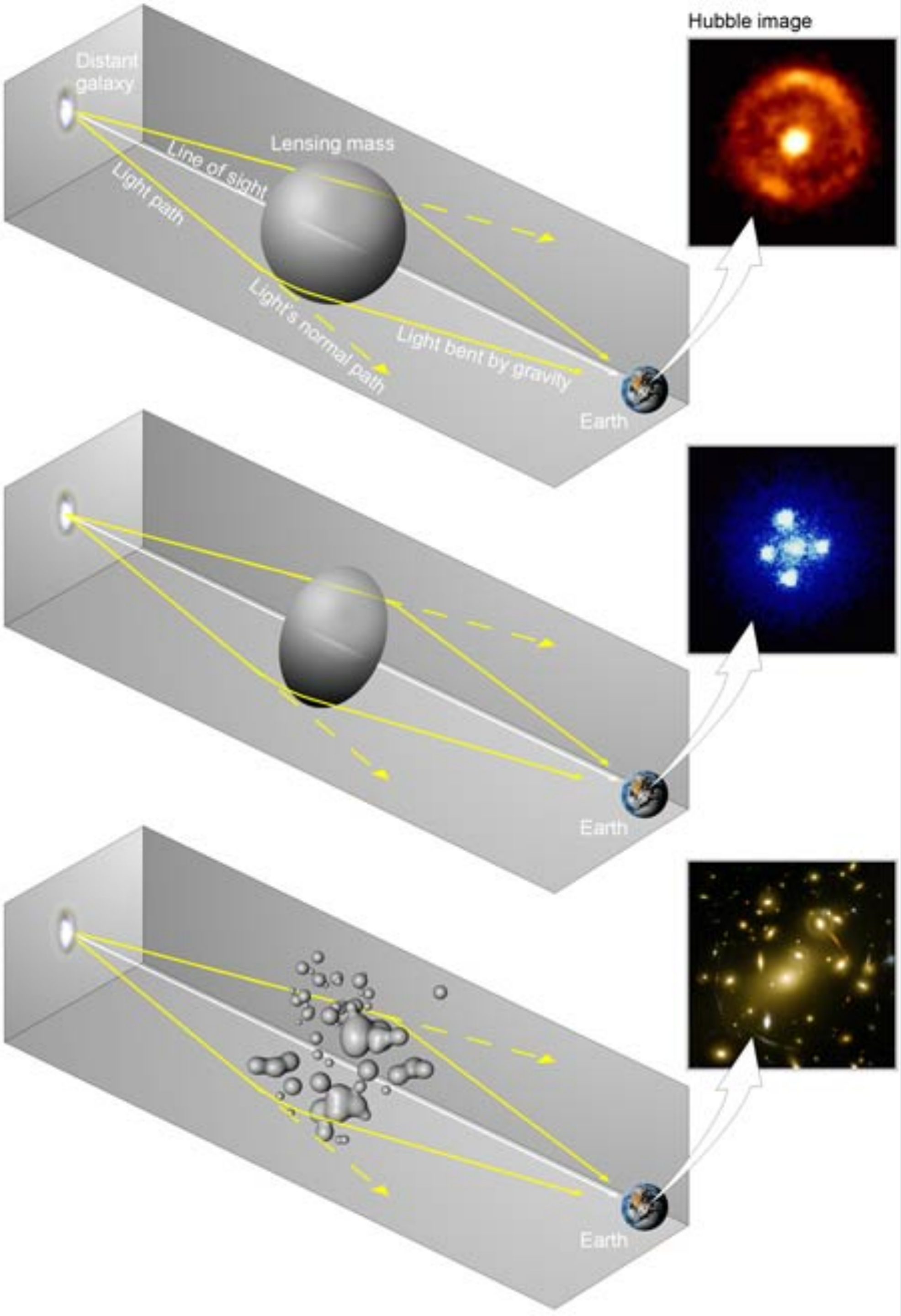
Hubble image
Distant galaxy
Lensing mass
Line of sight
Light path
Light's normal path
Light bent by gravity
Earth
Earth
Earth

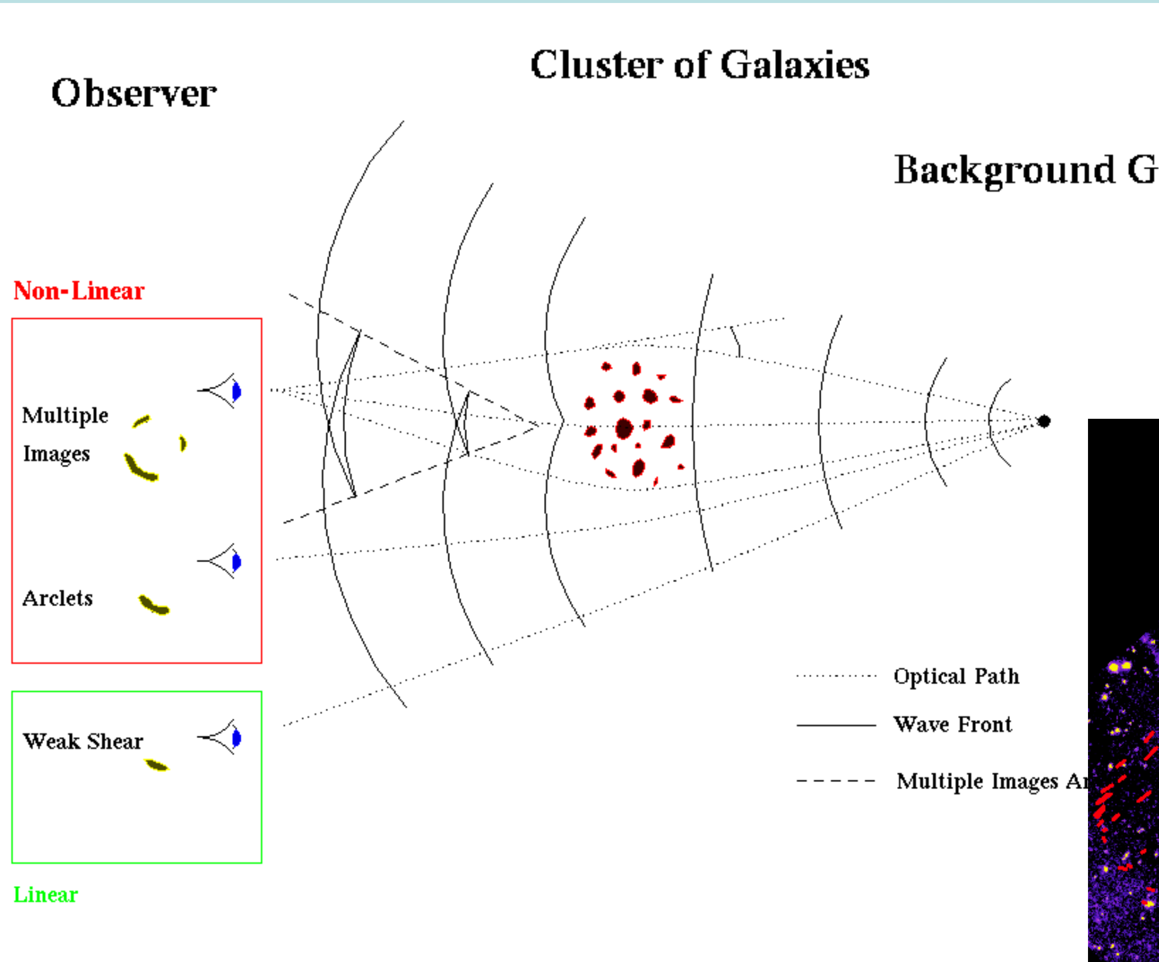
Observer
Cluster of Galaxies
Background Ga
Non-Linear
Multiple
Images
Arclets
Weak Shear
Linear
Optical Path
Wave Front
Multiple Images Ar

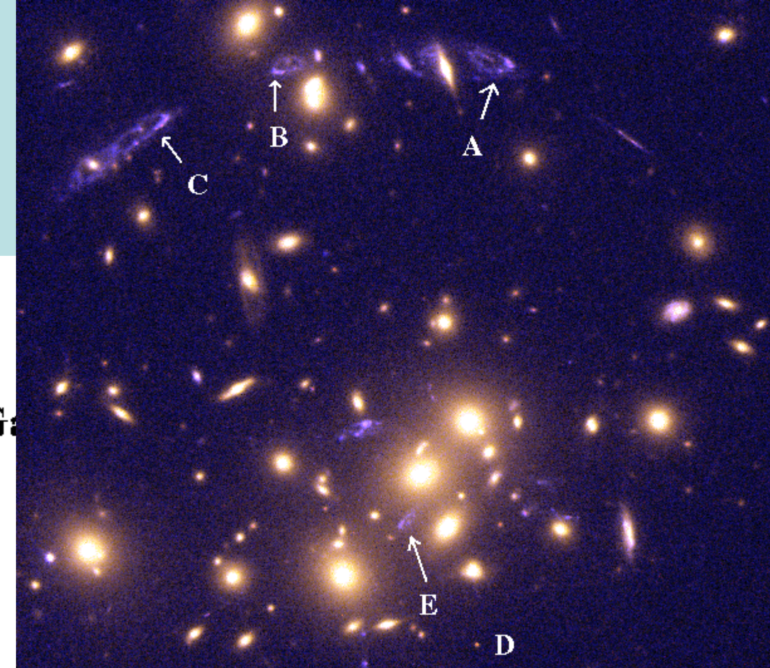
A
B
C
D
E

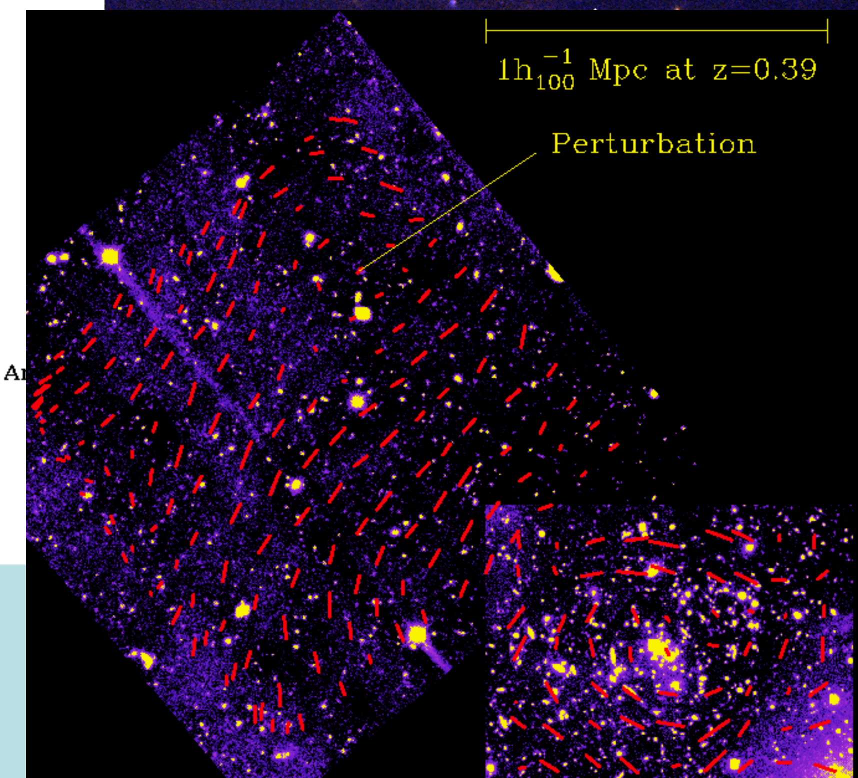
$1h_{100}^{-1}$ Mpc at z=0.39
Perturbation

Isotropic effect of lensing: magnification

multiple images, highly distorted and magnified arcs, dilution/depletion of background galaxy number counts

Projected surface mass density within the beam

$$\Sigma(r) > \Sigma_{crit}$$

Mass enclosed within the arc is tightly constrained

$$\Sigma_{crit} = \left[\frac{D_d D_{ds}}{D_s} / 1Gpc \right]^{-1} \times 0.35$$

$$\Sigma(q_{arc}) \approx \Sigma(q_E)$$

$$M(q_{arc}) = \Sigma_{crit} \times p \times \left(D_d q_{arc} \right)^2$$

Mass enclosed within the Einstein radius

Strong lensing

multiple images, highly distorted and magnified arcs, depletion of background number counts

- Projected surface mass density within the beam $\Sigma(r) > \Sigma_{crit}$
- Mass enclosed within the arc is tightly constrained

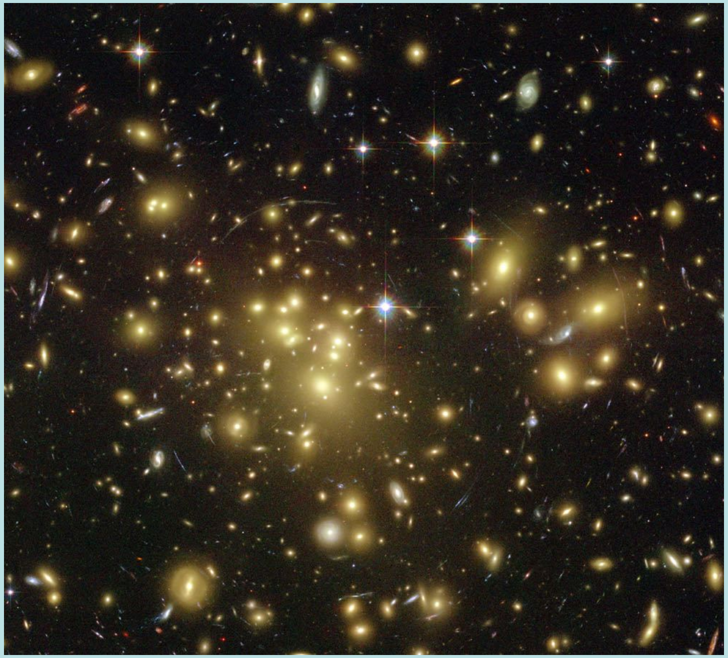

Weak lensing

coherent distortion in the shapes of background galaxies

- Shear field used to construct mass map

Kaiser & Squires 93

Mapping DM in clusters

DM potential = 'smooth' component + clumps

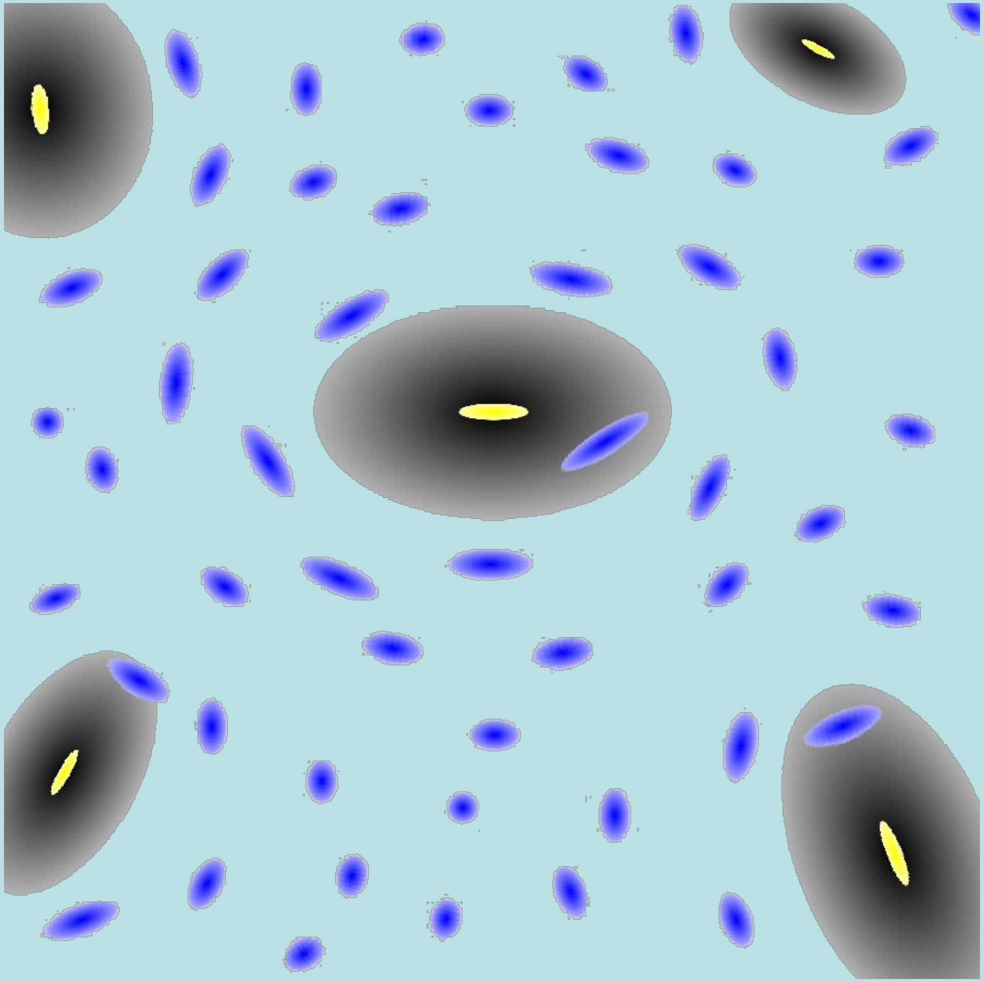

Mass modeling

Galaxy Cluster Abell 2218

Hubble Space Telescope • WFPC2

A. Fruchter and the ERO Team (STScI, ST-ECF) • STScI-PRC00-08


R = 6.0 Mpc
z = 10.155
a = 0.090
diemand 2003

The power of substructure mapping

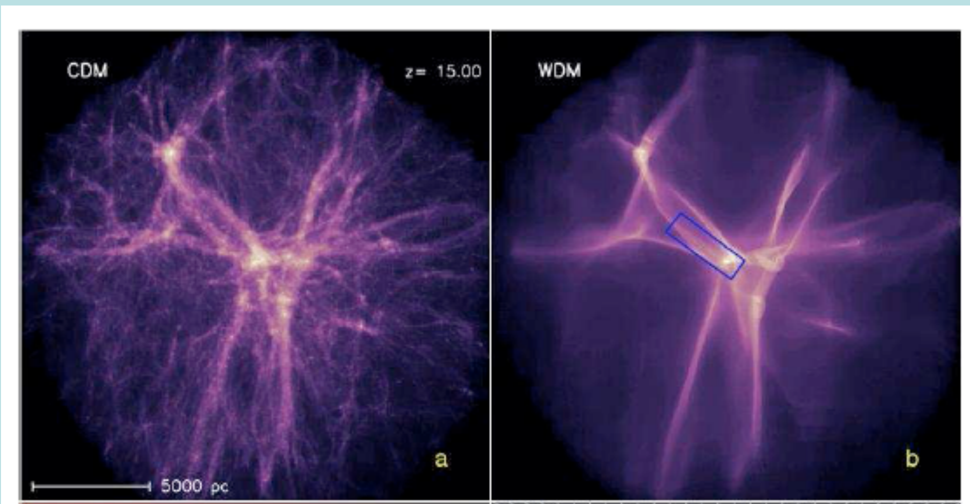

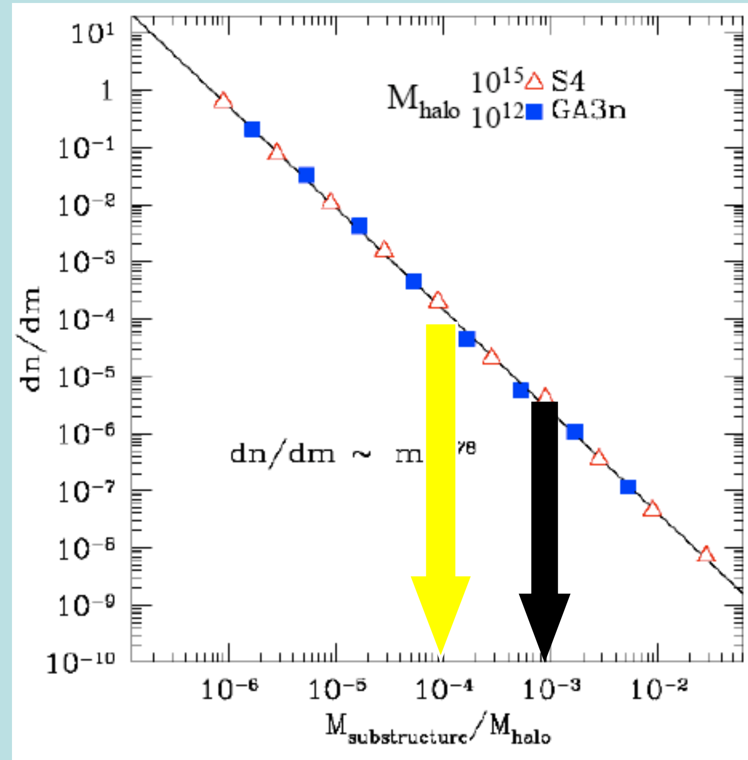

dependence on the nature of DM

Very weak dependence on halo mass

Gao & Theuns 2007; PN & Kuhlen 2013

MAPPING SUBSTRUCTURE IN CLUSTERS

$$\Phi_{cluster} = \sum_i \Phi_{smooth} + \sum_n \Phi_{perturbers}$$

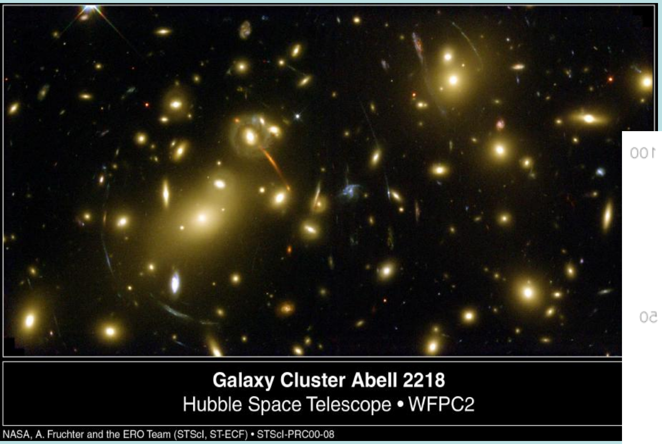

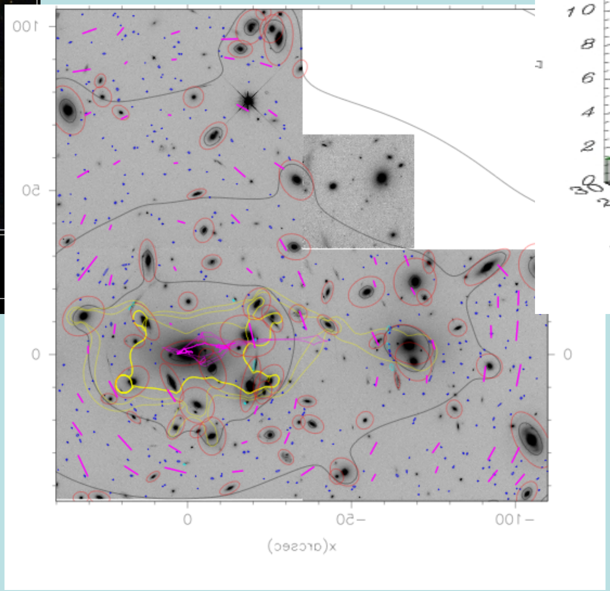

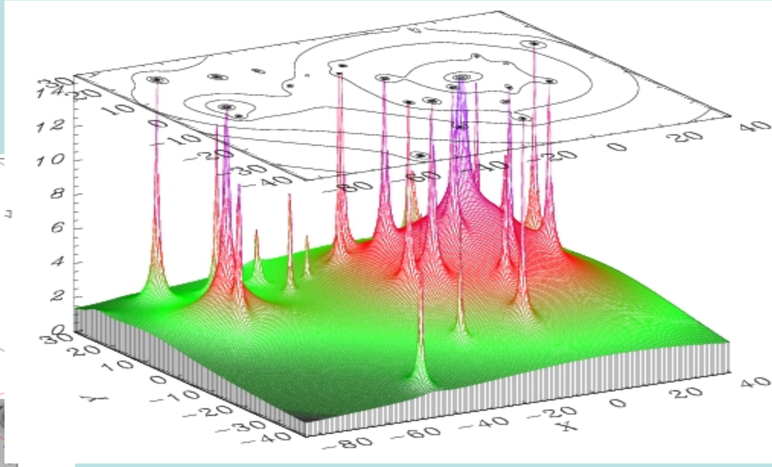

PN & Kneib 1997; PN+ 2005; 2009; 2011

Sub-halo properties

- cut radii; mass, velocity dispersion; M/L ratios; mass function; radial distribution

$$r_{core} = r^*_{core} \left(\frac{L}{L^*}\right)^{\frac{1}{2}} \quad r_{cut} = r^*_{cut} \left(\frac{L}{L^*}\right)^{\alpha} \quad \sigma = \sigma^* \left(\frac{L}{L^*}\right)^{\frac{1}{4}}$$

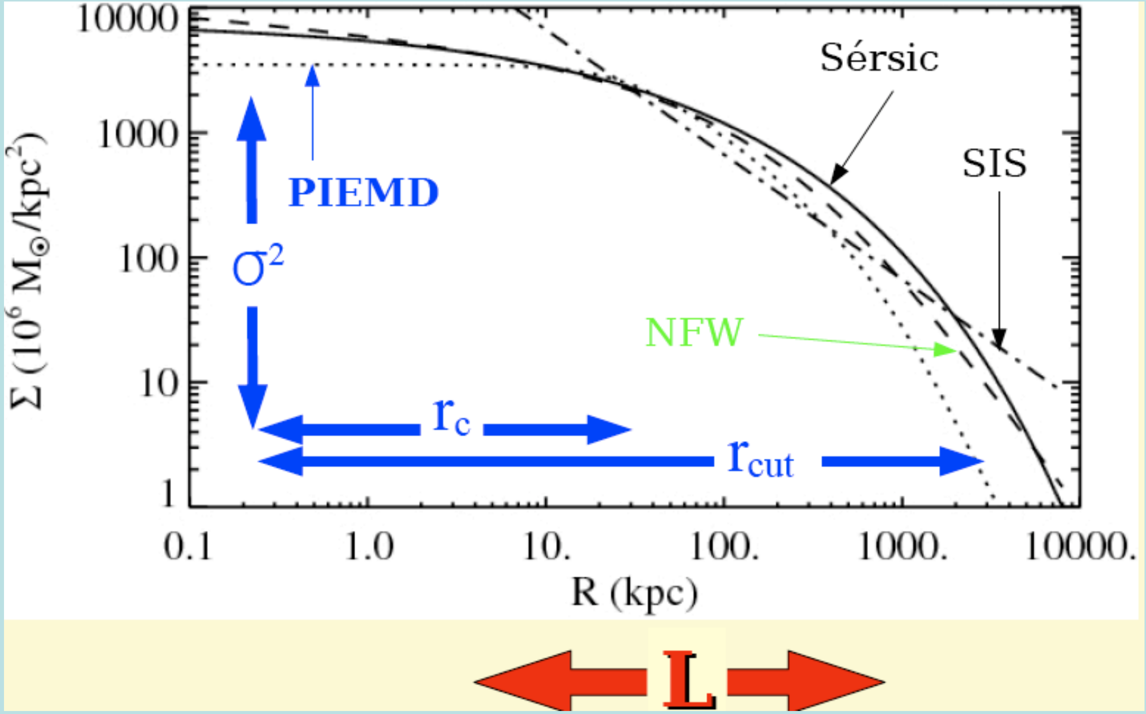

The detailed dark matter distribution in A2218

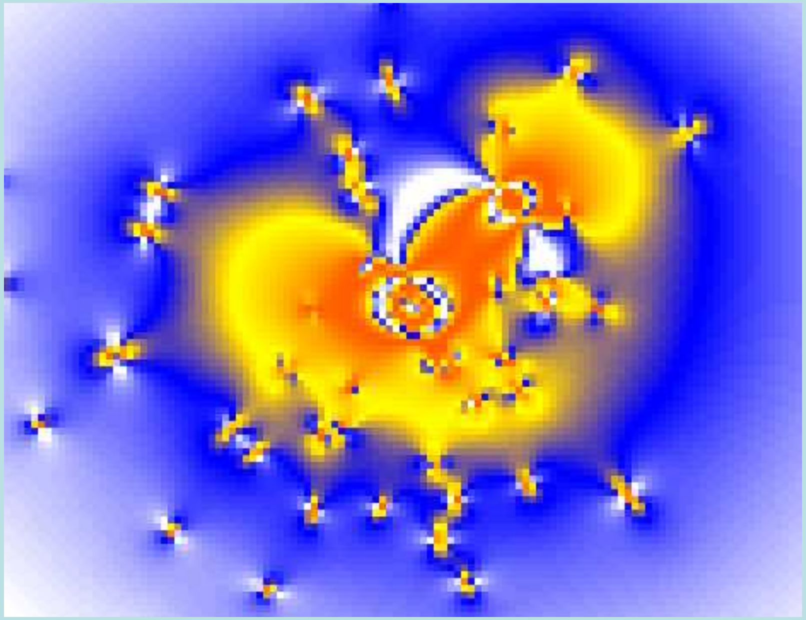

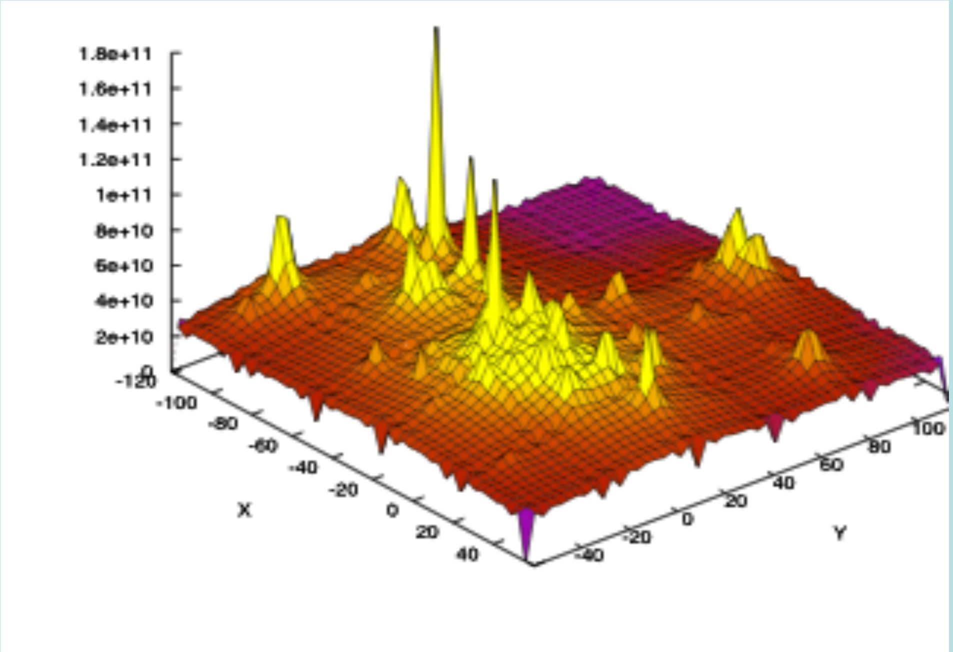

PN+ 04; 05; 06

Cl0024+16 extending analysis to 5 Mpc

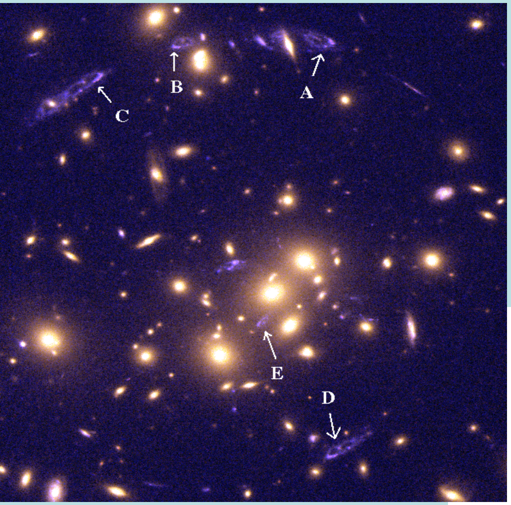

HST wide field sparse mosaic
76 orbits, 38 pointings

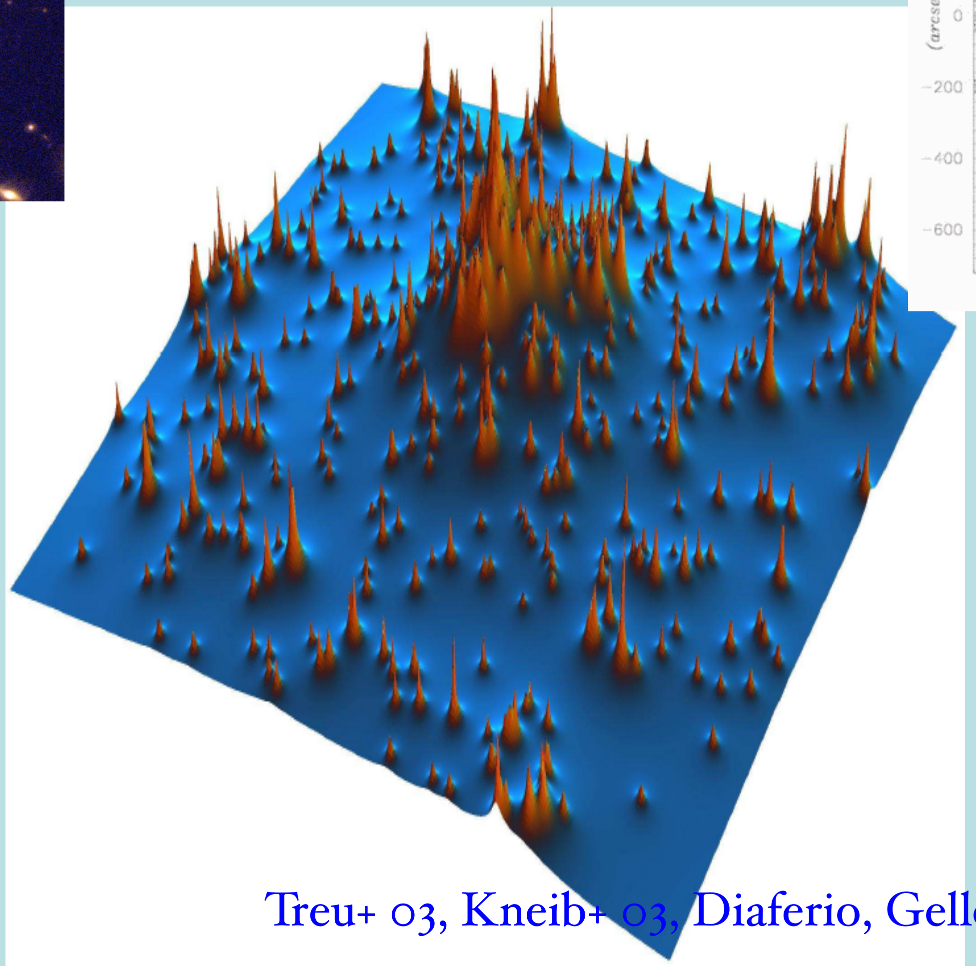

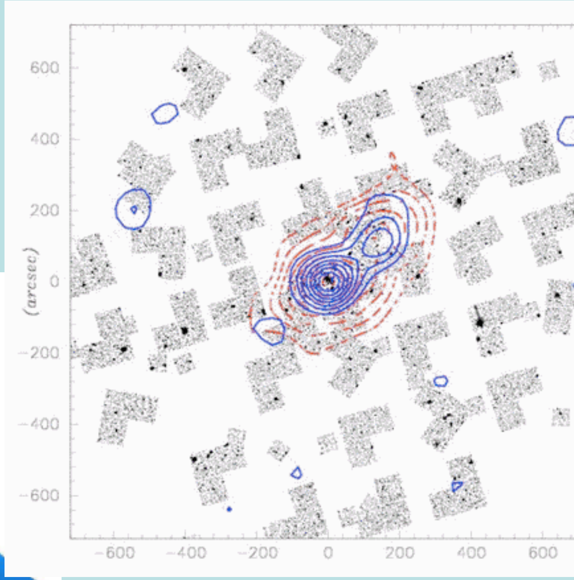

Treu+ 03, Kneib+ 03, Diaferio, Geller & Rines 05; PN+ 09

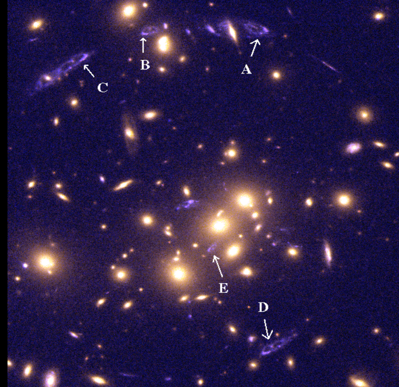

A
B
C
D
E

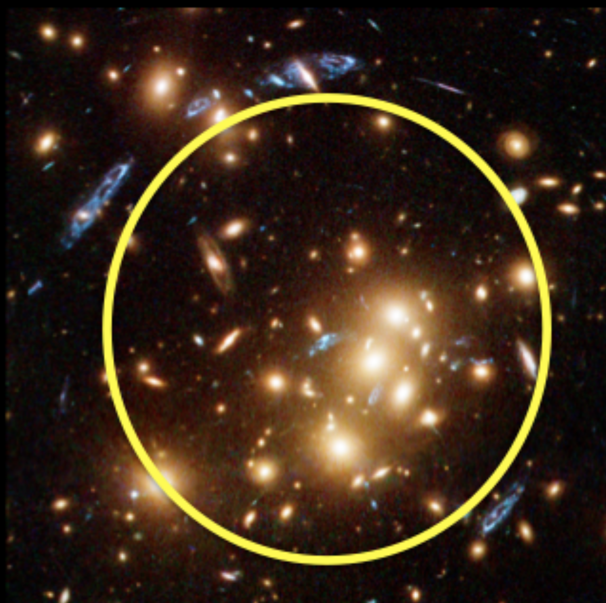

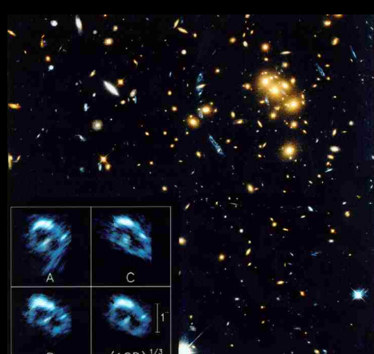

A
C
D
(ACD)1/3

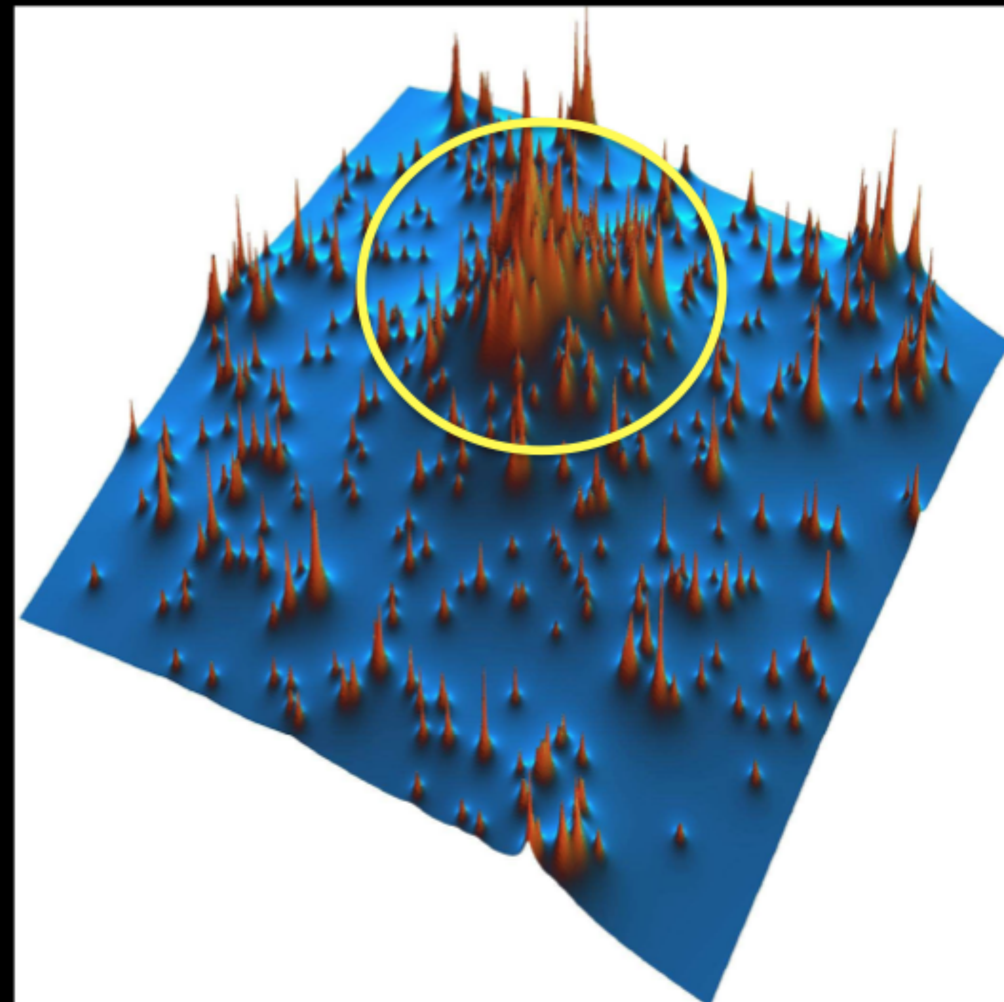

Granularity of DM - substructure

dependence on the nature of DM

$$\frac{dn}{dm} \propto m^{-1.8}$$

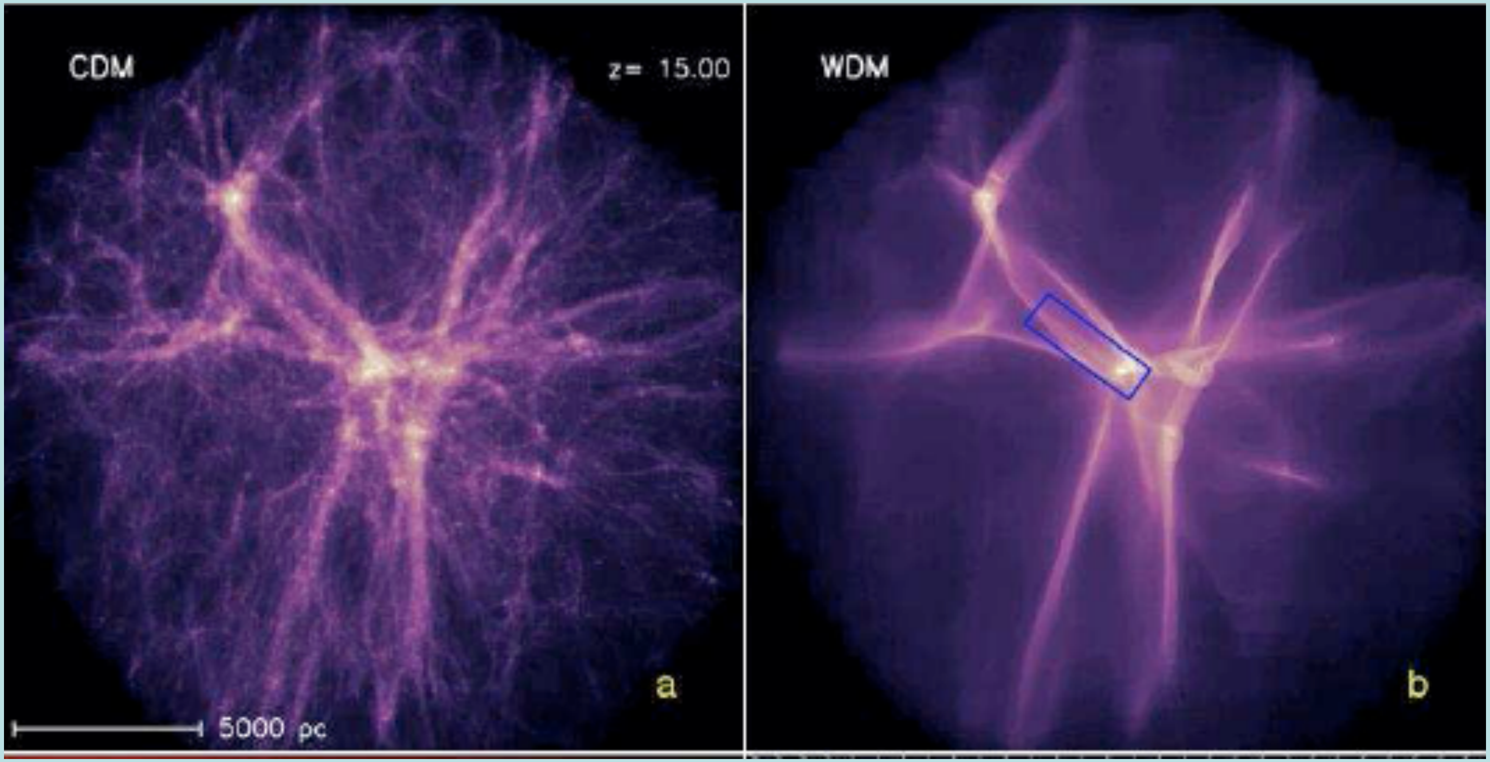

Springel+ 05; PN, De Lucia & Springel 07; Gao & Theuns 2007; PN+09,12, 17

Comparison with LCDM clusters in the Millenium Run

The subhalo mass function

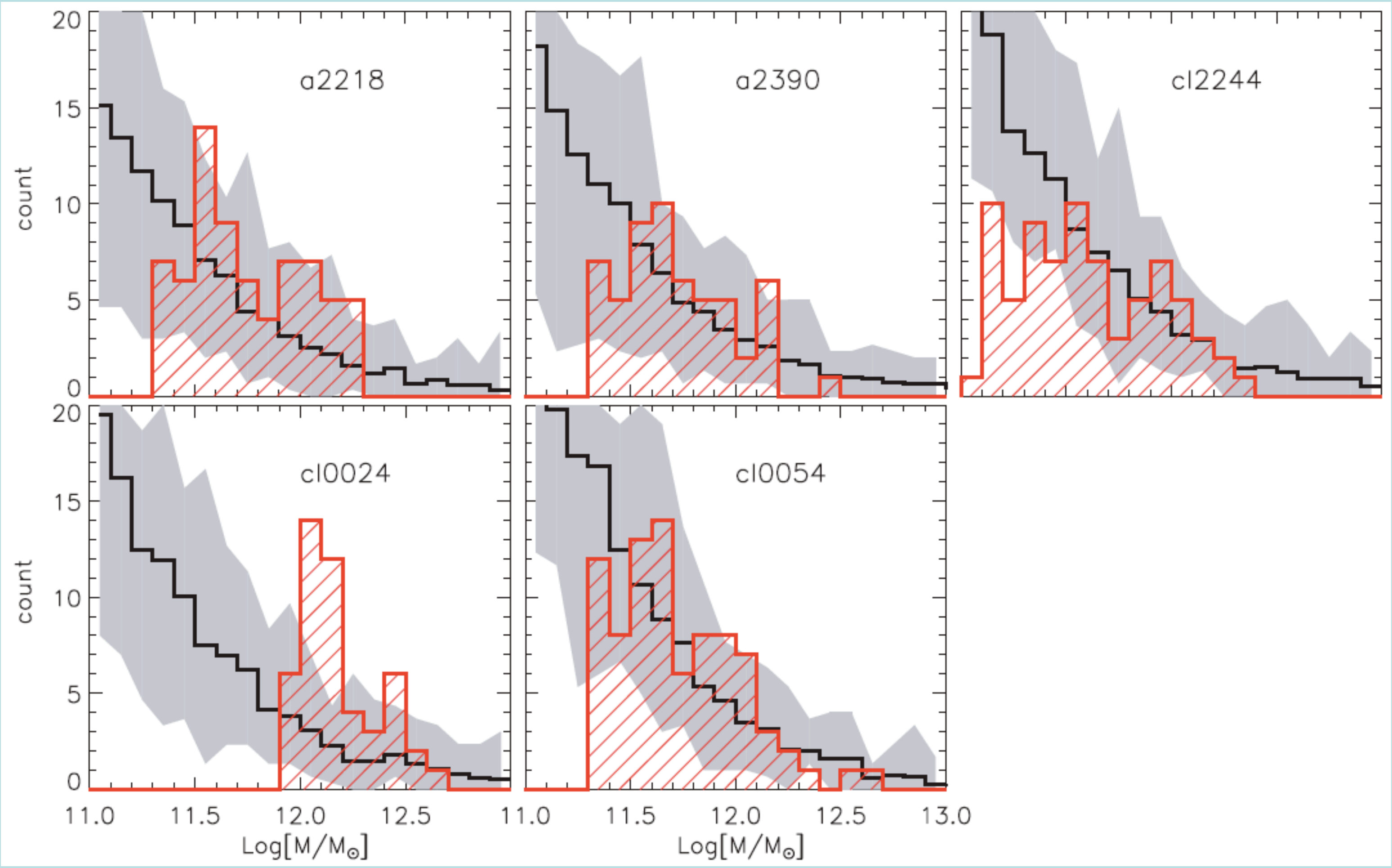

Springel+ 05; PN, De Lucia &
Springel 07; PN+ 09, 12, 17

HST Frontier Fields

P.I. Matt Mountain, Jen Lotz

http://www.stsci.edu/hst/campaigns/frontier-fields

HUBBLE FRONTIER FIELDS

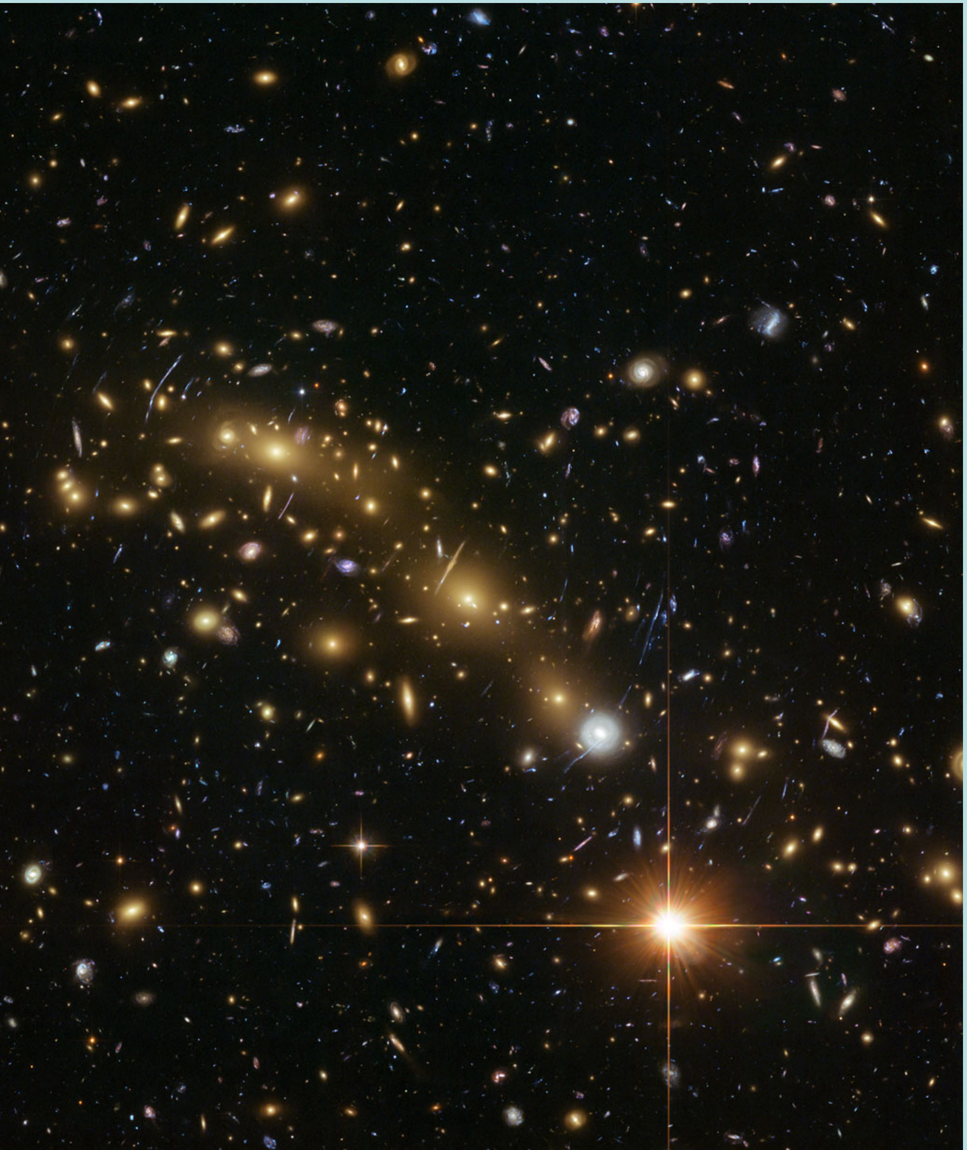

Mapping substructure with the HST Frontier Fields

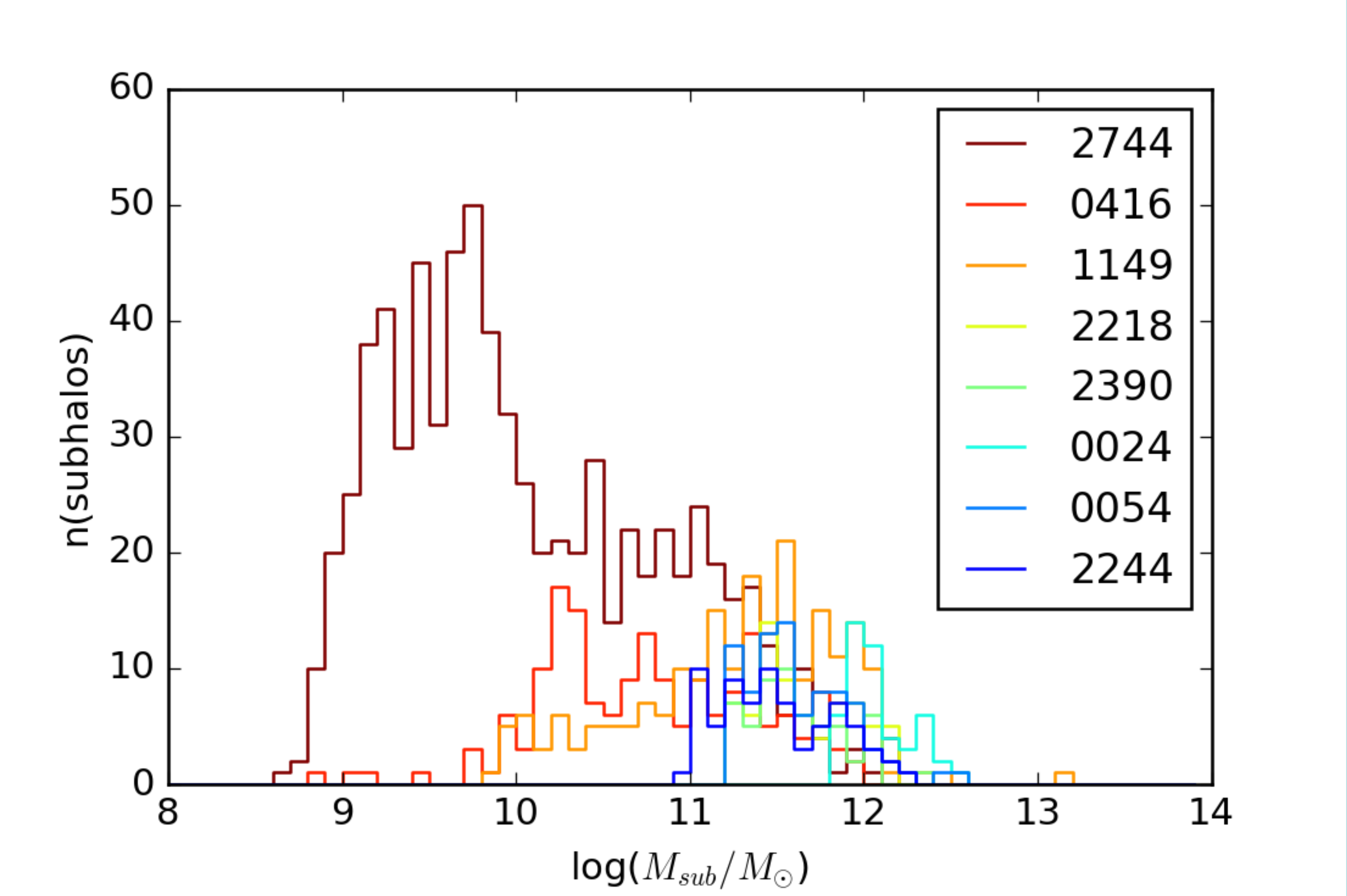

BEST FIT MODEL: d.o.f – 139, chi²=2.04 and RMS = 0.69"

51 image families, 159 images, 2 large scale PIEMDs + 733 cluster galaxies

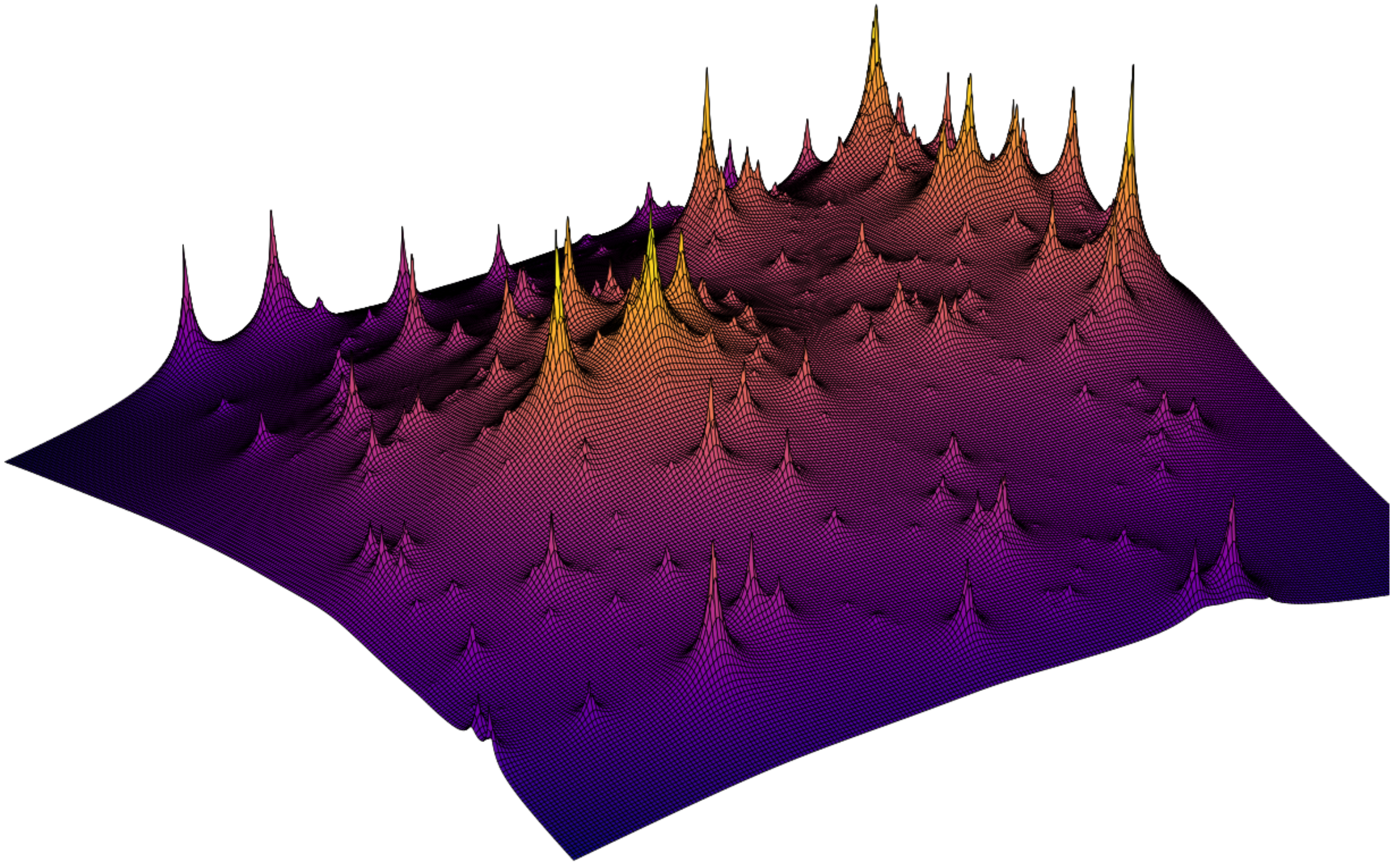

ILLUSTRIS

AREPO MOVING MESH CODE

DM ONLY RUN
FULL PHYSICS RUN

name	volume [(Mpc)^3]	DM particles / hydro cells / MC tracers	$\epsilon_{baryon}/\epsilon_{DM}$ [pc]	m_{baryon}/m_{DM} [10^5 $M_\odot$]	r_{cell}^{min} [pc]
Illustris-1	106.5^3	$3 \times 1,820^3 \cong 18.1 \times 10^9$	$710/1,420$	$12.6/62.6$	48
Illustris-2	106.5^3	$3 \times 910^3 \cong 2.3 \times 10^9$	$1,420/2,840$	$100.7/501.0$	98
Illustris-3	106.5^3	$3 \times 455^3 \cong 0.3 \times 10^9$	$2,840/5,680$	$805.2/4008.2$	273
Illustris-Dark-1	106.5^3	$1 \times 1,820^3$	$710/1,420$	$-/75.2$	–
Illustris-Dark-2	106.5^3	1×910^3	$1,420/2,840$	$-/601.7$	–
Illustris-Dark-3	106.5^3	1×455^3	$2,840/5,680$	$-/4813.3$	–

The initial conditions assume a LCDM cosmology consistent with WMAP-9 measurements, from which a linear power spectrum is used to create a random realization in a periodic box with side length 75 Mpc/h = 106.5 Mpc, at a starting redshift of 127. A series of simulations are run at different resolutions, and a second set is run with only dark matter. The main simulation initially has 1820^3 = 6,028,568,000 hydrodynamic cells, and the same number of DM particles and MC tracers (see table for more details, including mass resolutions and gravitational softening lengths). Evolving the main simulation to z=0 used 8,192 compute cores, a peak memory of 25 TB, and 19 million CPU hours.

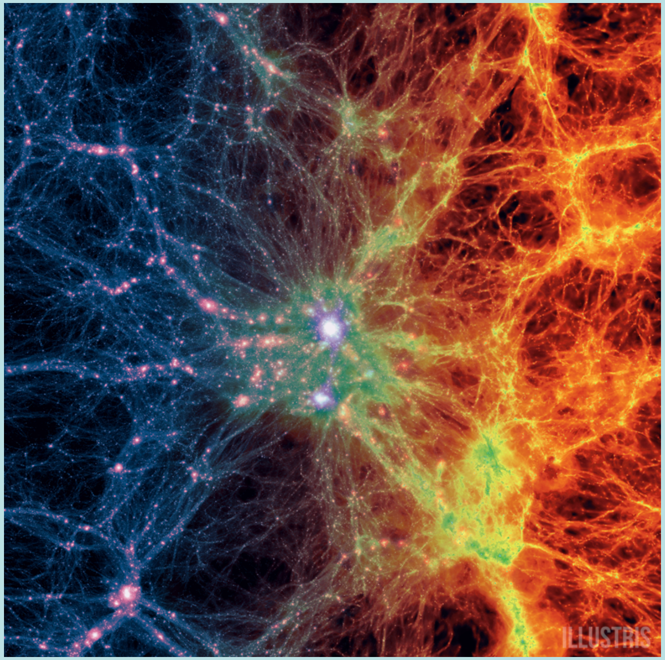

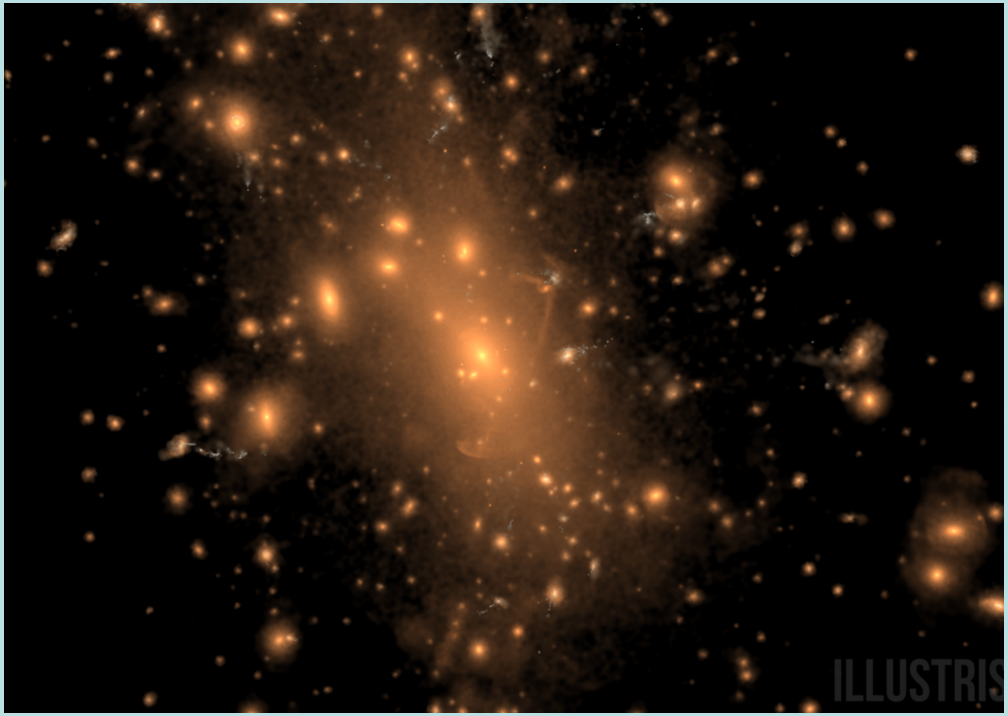

Comparison with Illustris zoom LCDM clusters

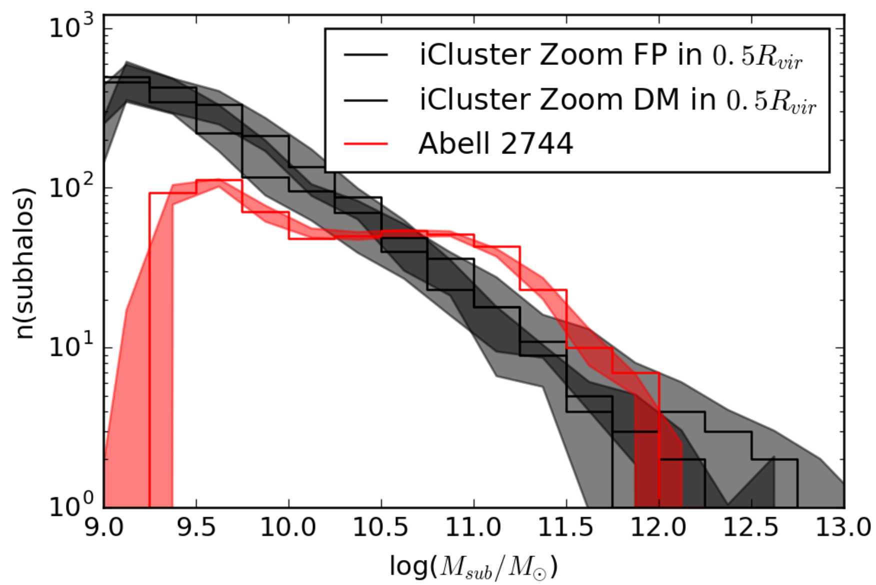

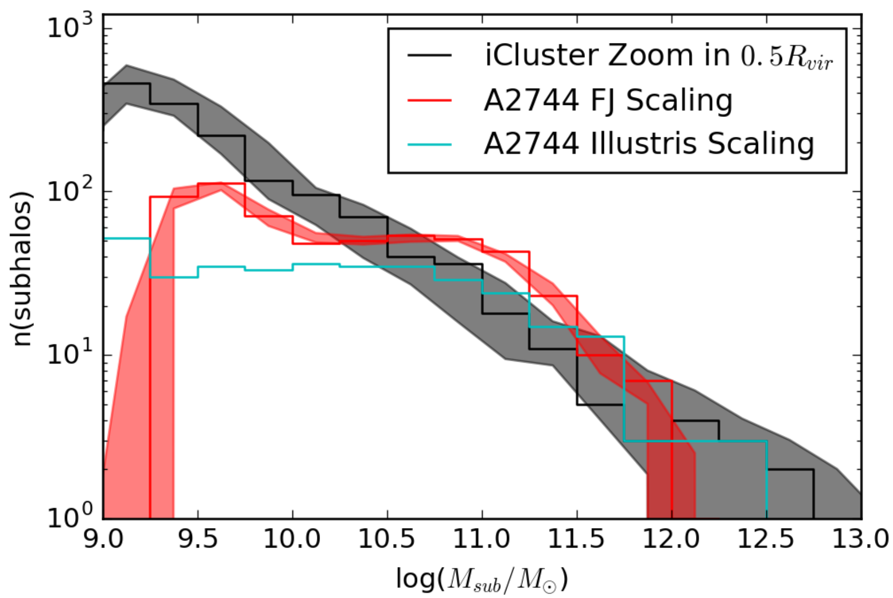

The subhalo mass function

PN+ 2017

Comparison with Illustris LCDM clusters

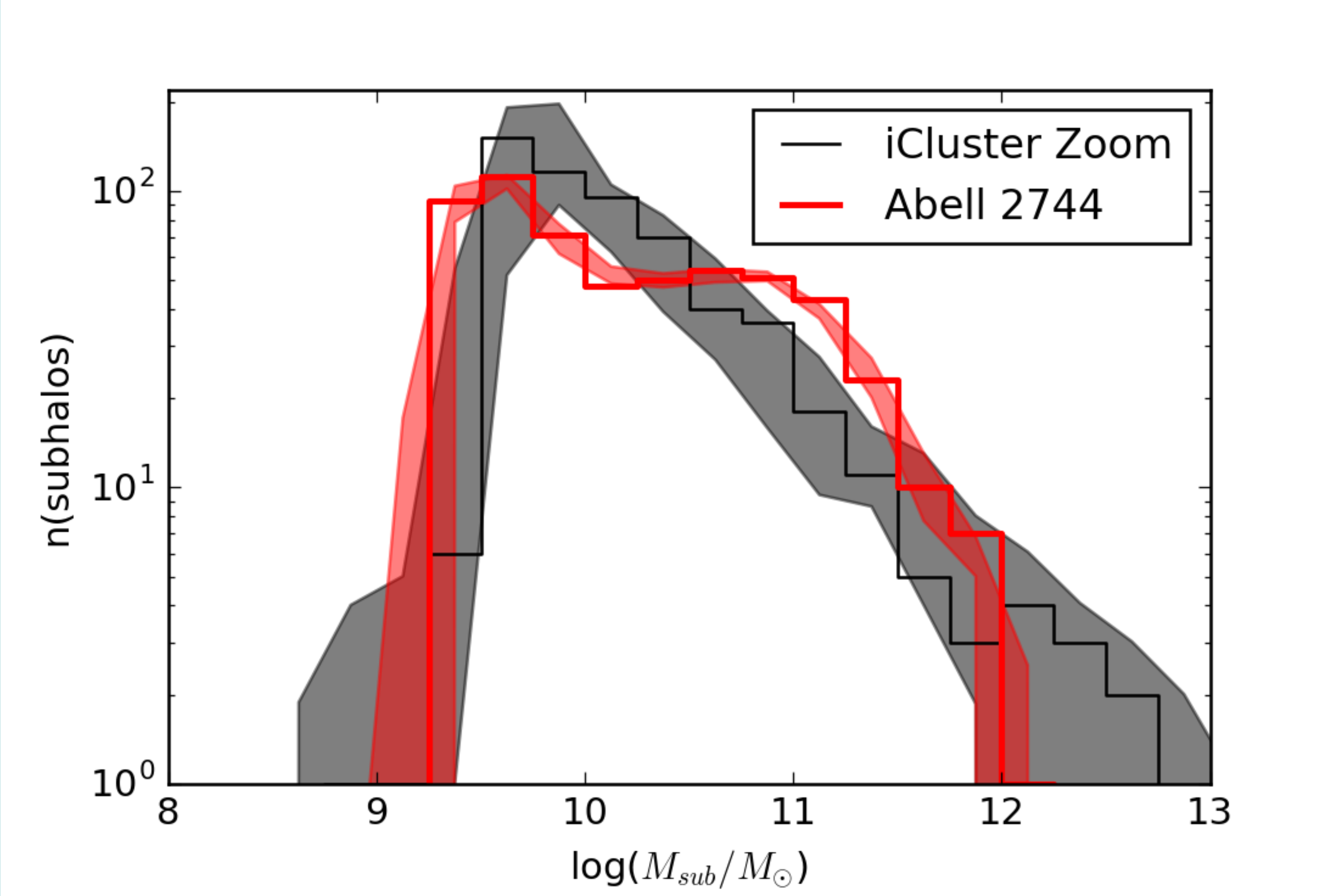

The subhalo mass function

Comparison with Illustris LCDM clusters

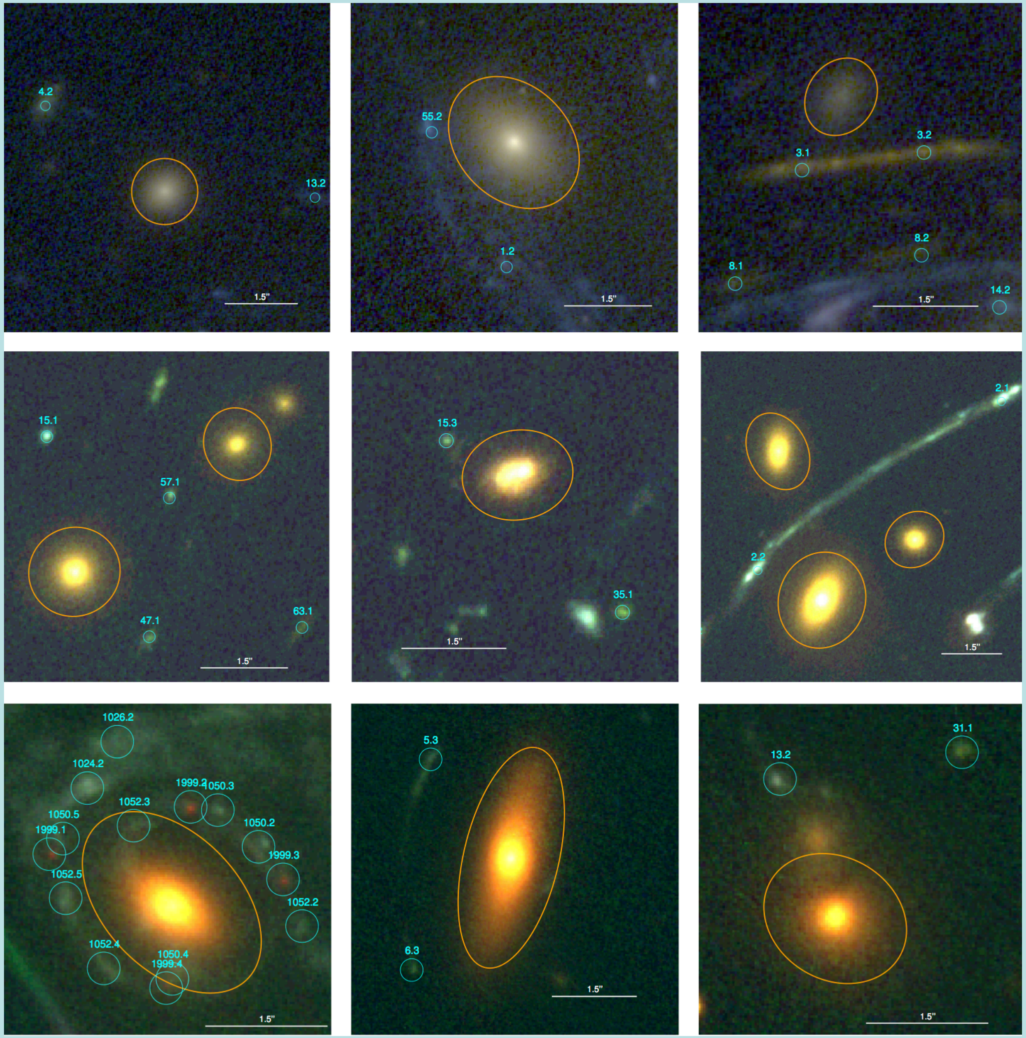

Comparison with Illustris LCDM clusters

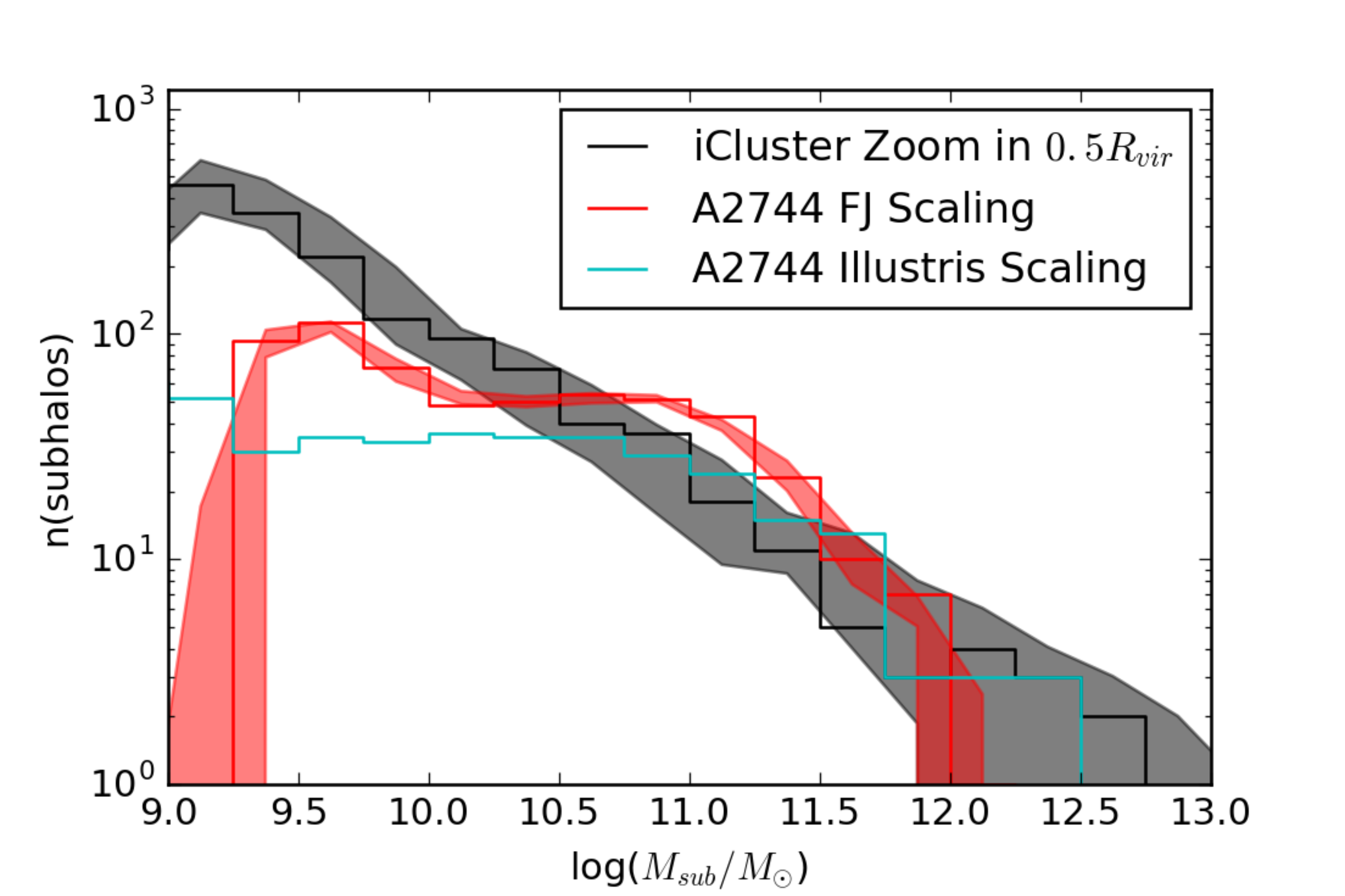

The subhalo mass function

PN+ 17

Comparison with Illustris LCDM clusters

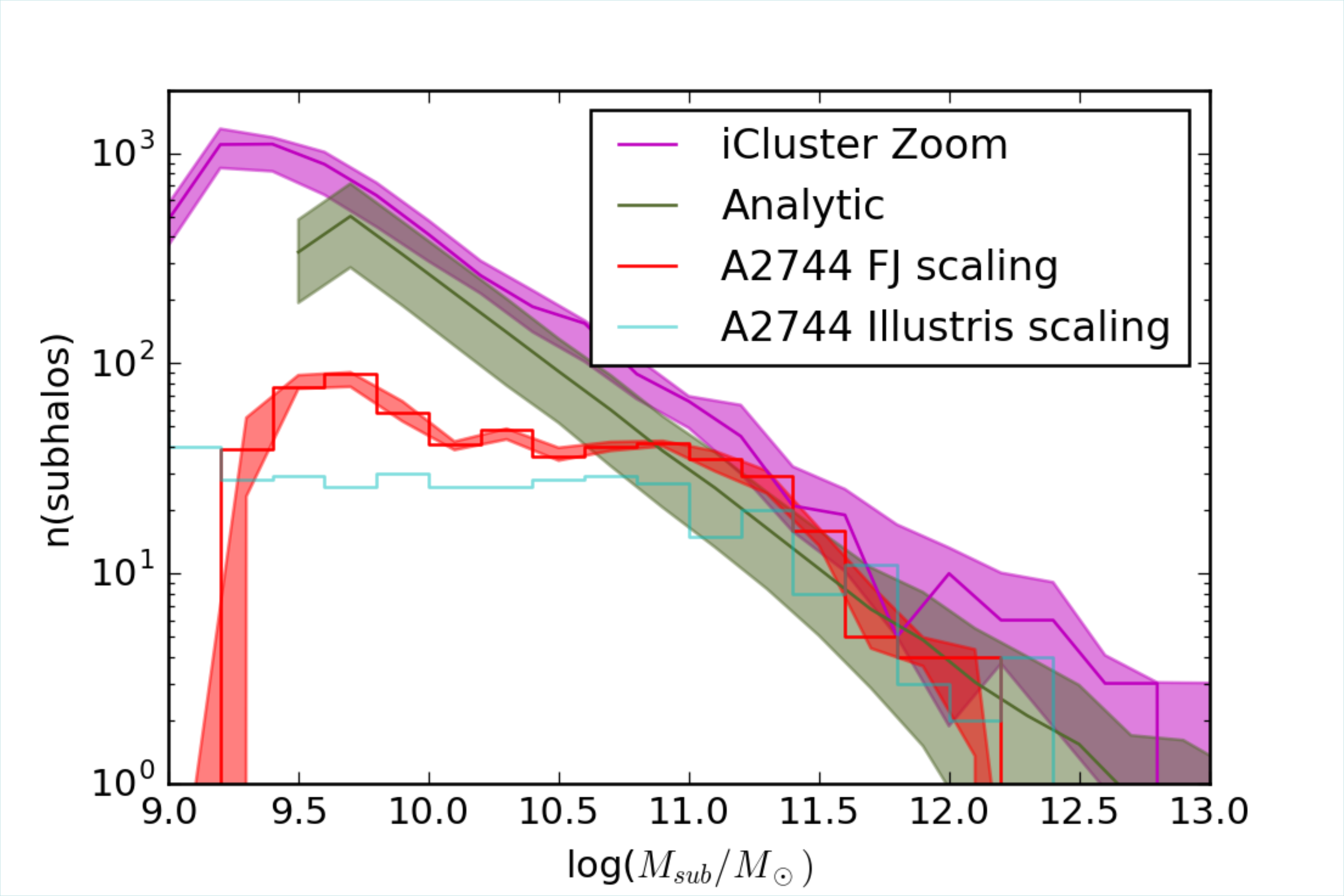

The subhalo mass function

PN+ 17

Comparison with Illustris LCDM clusters

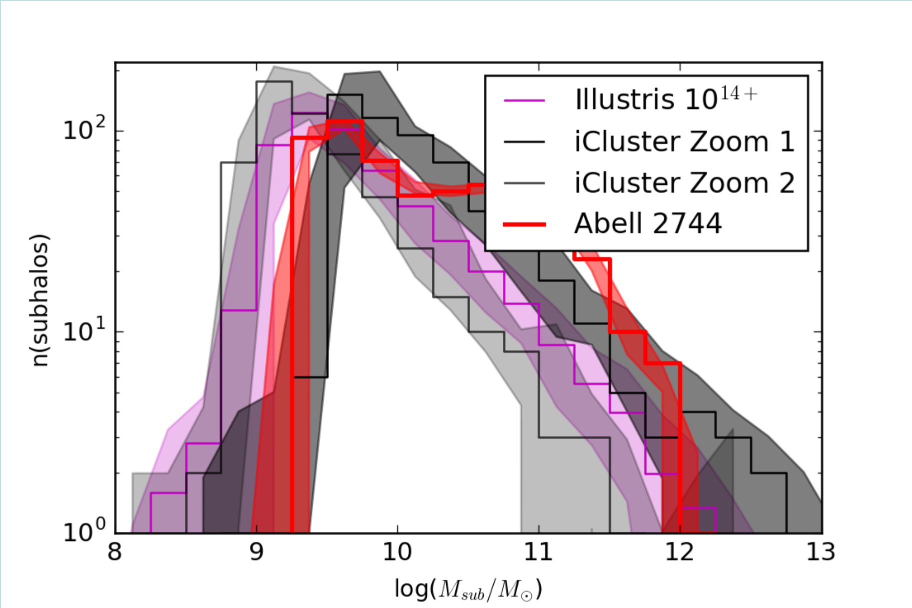

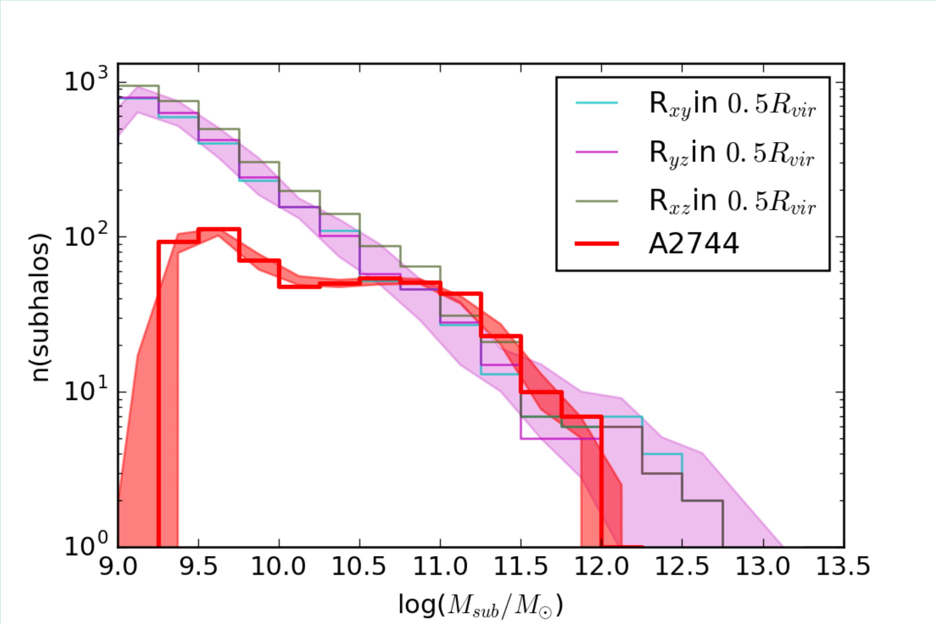

The subhalo mass function

PN+ 17

Comparison with Illustris LCDM clusters

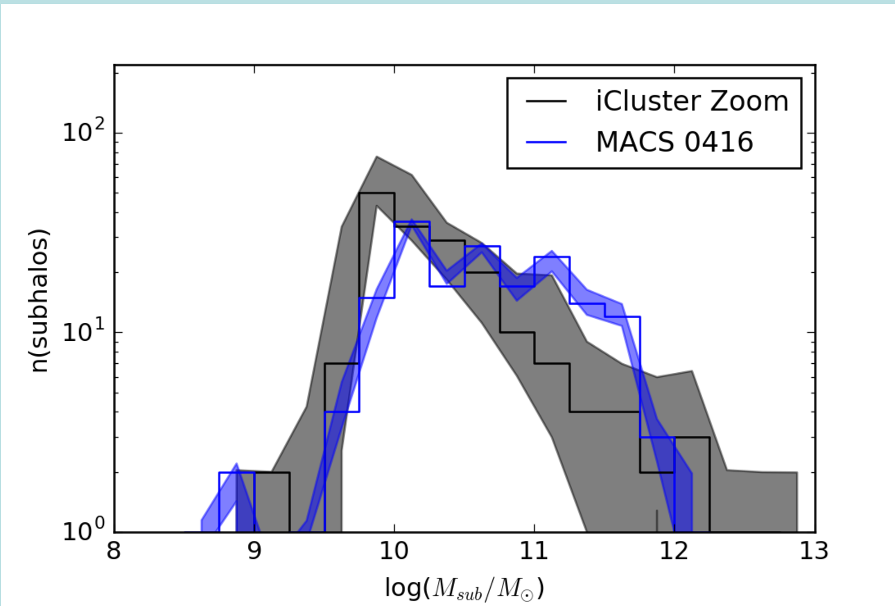

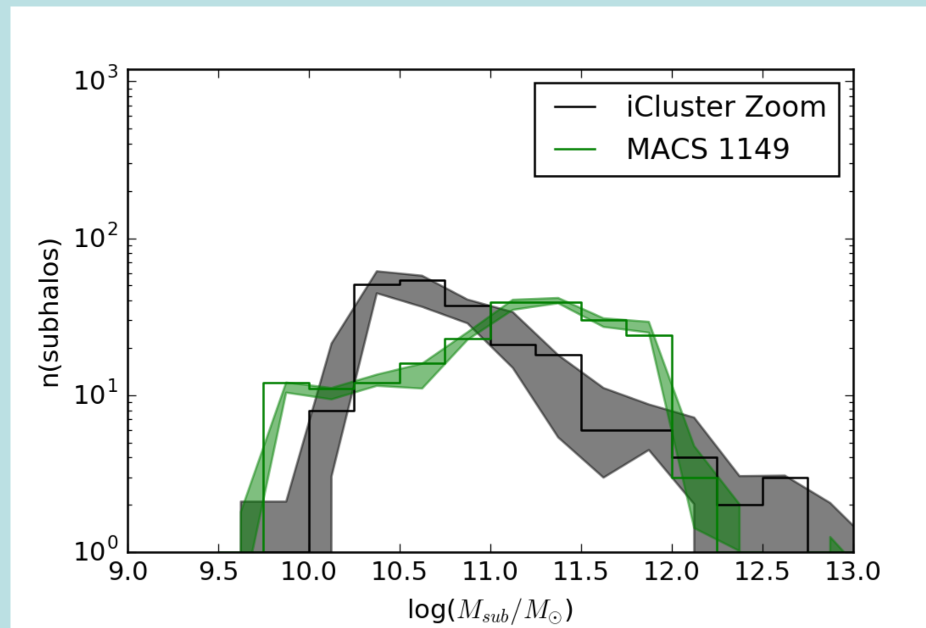

The subhalo mass function

PN+ 17

THE SUBHALO MASS FUNCTION

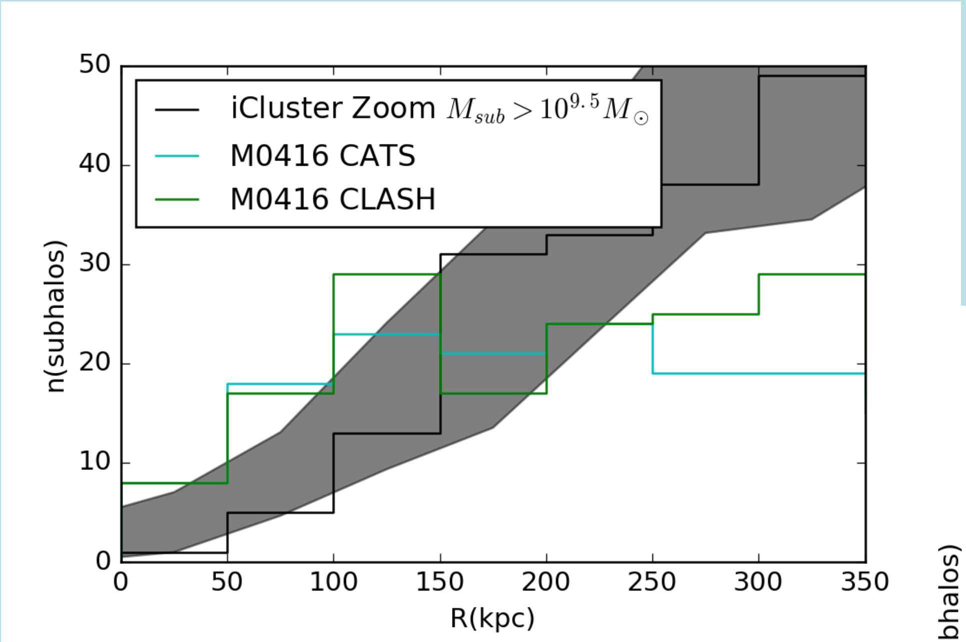

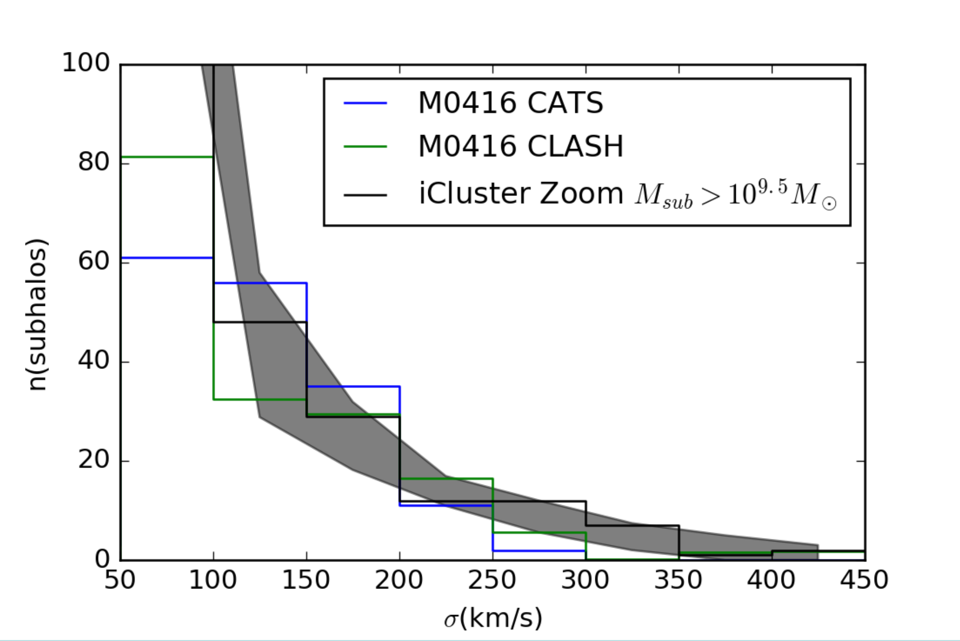

Comparison with Illustris LCDM clusters
only tension with LCDM

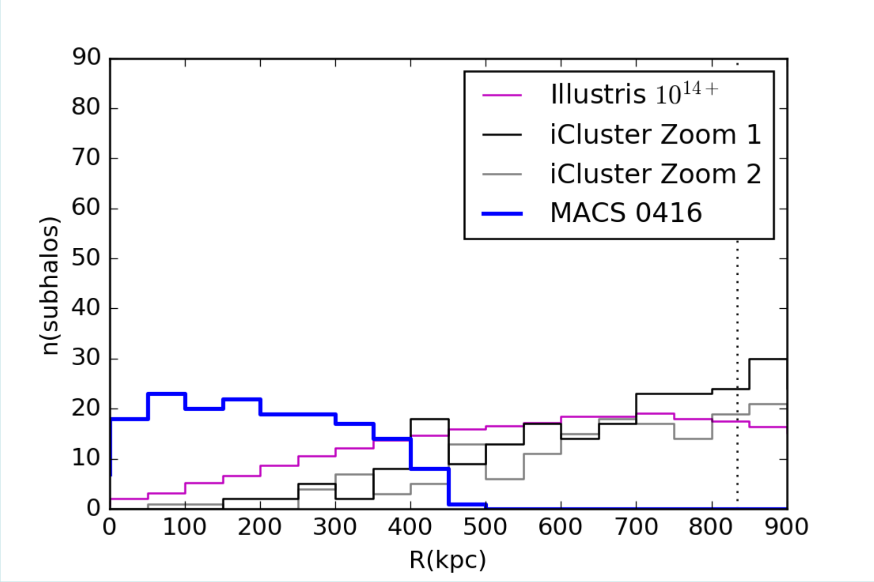

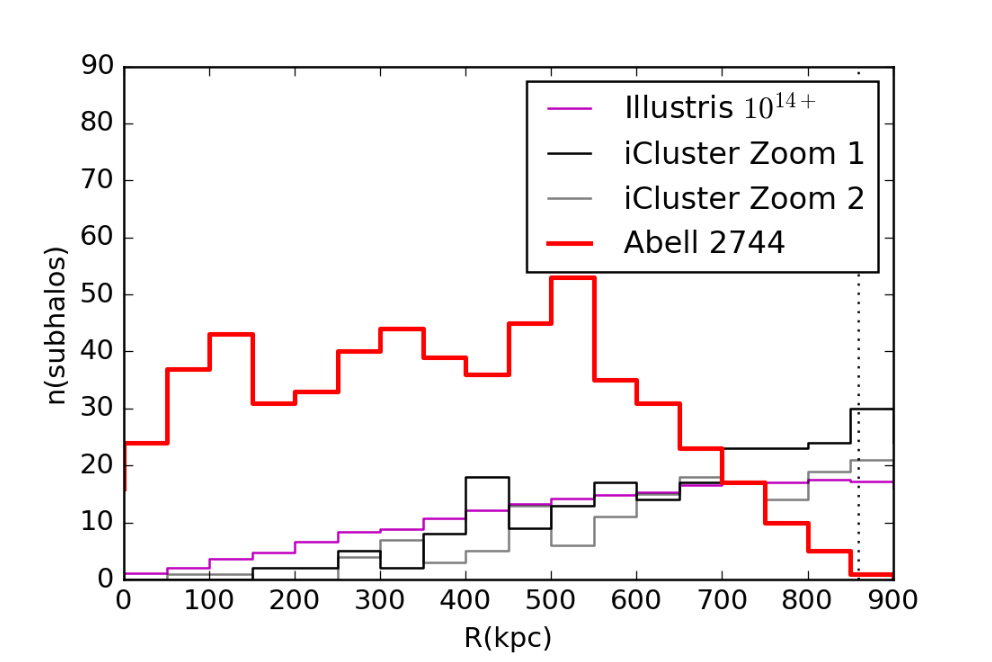

Radial distribution of subhalos

PN+ 17

Testing the LCDM paradigm

LOW ACCELERATION REGIME $a < a_0 \sim 10^{-10}$ m s^{-2}

$$g_{tot}(r) = V^2_{circ}(r)/r \quad ; \quad g_{bar}(r)$$

$$g_{tot} \sim g_{bar} \text{ when } g_{tot} > a_0$$

- Disk galaxy rotation curves show clear and marked deviation from the Newtonian predictions **only in this regime**

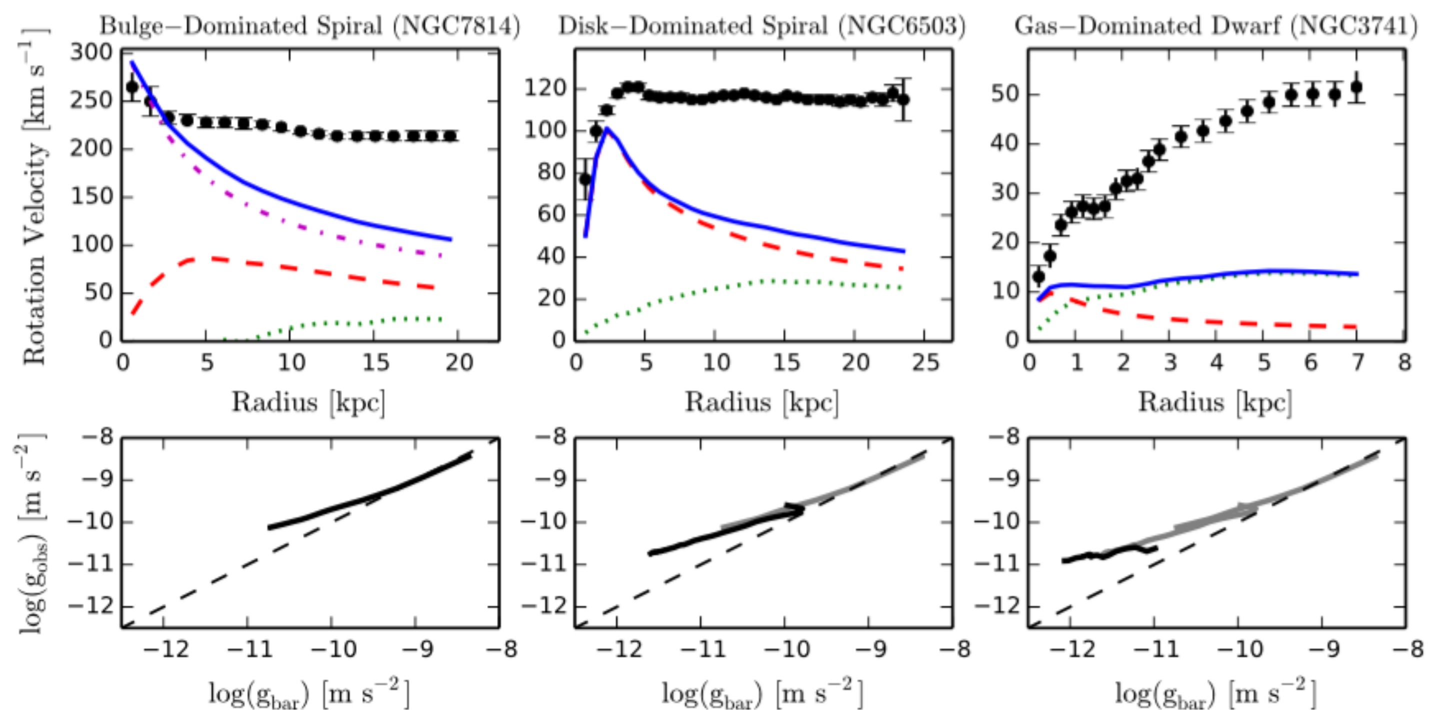

Testing the LCDM paradigm

Arises naturally in LCDM

(i)Due to inside-out formation of galaxies
(ii) Acceleration profiles in LCDM self-similar
(iii) Disk size & halo mass scale with baryonic mass

MNRAS **000**, ??–?? (2016) Preprint 11 January 2017 Compiled using MNRAS LaTeX style file v3.0

The origin of the mass discrepancy-acceleration relation in ΛCDM

Julio F. Navarro[1*], Alejandro Benítez-Llambay[2], Azadeh Fattahi[1],
Carlos S. Frenk[2], Aaron D. Ludlow[2], Kyle A. Oman[1], Matthieu Schaller[2],
Tom Theuns[2].

An optimist's tally of lensing tests of cold dark matter

Substructure: mass function of DM halos, spatial distribution of DM halos agree well

Density profiles of DM halos: profile outer slopes consistent with NFW ($< r_{vir}$), inner slopes unclear but appear to be consistent with no cores, some dispersion

Tidal stripping: galaxy orbits and dynamics - reasonable agreement complicated by baryons; collisionless DM favored over fluid models

Lensing cross-sections and arc statistics: good agreement at low z, hints of excess at z > 0.6

super-lenses, structure along the line of sight

Concentration-Mass relation: in agreement within errors of the relation seen in LCDM simulations